AMERICAN REVOLUTION BICENTENNIAL 1776-1976

office of

NAVAL RESEARCH

REVIEWS

MARCH 1976

DEPARTMENT OF THE NAVY · OFFICE OF NAVAL RESEARCH

PROFILES IN SCIENCE

Dr. Nick Paul Fofonoff

Dr. Nick Paul Fofonoff is a physical oceanographer, Senior Scientist at Woods Hole Oceanographic Institution and The Professor of the Practice of Physical Oceanography at Harvard University. He has been an ONR principal investigator since 1963. Dr. Fofonoff is best known for his two lengthy and scholarly articles on physical and thermodynamic properties of sea water and the dynamics of ocean currents which appeared in *THE SEA: Ideas and Observations*, Volume 1, 1962. His research interests also include the application of moored buoy systems to measurement of ocean currents. Dr. Fofonoff served as the Chairman of the Department of Physical Oceanography at Woods Hole from 1967-71. He has been the principal scientist directing the famous Woods Hole Buoy Group. He has been instrumental in helping many young physical oceanographers to understand the important problems in oceanography. He is a key member of several international panels and serves on the POLYMODE Executive committee.

Physical Oceanography Program in ONR

James O'Brien
Office of Naval Research

As military technology has advanced and become more complex, military operations have become even more sensitive to the environment. To meet its future demands for specific and reliable forecasting of environmental conditions affecting its operations at sea, the Navy requires a comprehensive base of knowledge about the processes controlling the variability of the physical structure of the ocean's water. The Office of Naval Research's Physical Oceanography Program focuses on the quantification and understanding of the variability of the real-world ocean environment, its boundaries, and its associated sound field. It excludes the measurement and survey of the variable parameters without concurrent effort to understand the processes involved.

Recently, ocean variability has come into sharp focus. No longer is the ocean believed to be static in any of its properties; in fact, data collected over the last few years by ships, moored arrays, buoys, and satellites indicate just the opposite. Therefore, oceanographic atlases portraying mean climatic conditions, like their meteorological counterparts, should be used only to afford the zero orders estimates for values which have a large spread about the mean, often amounting to an order of magnitude. The concept of variability is by no means new, but the accent on variability and long-period problems has now become important because:

1. Observations in both atmosphere and ocean are taken routinely, and modern data-processing facilities are able to cope with millions of data with relatively easy storage and retrieval.

2. New knowledge of the general circulation of the atmosphere and oceans gained over the last 20 years together with modern synoptic observation capabilities makes complex air/sea coupling problems more tractable than before.

The Program is emphasizing the exchange of energy and mass between the atmosphere and the oceans, with particular attention to those exchange processes that effect naval operational capabilities. These include the propagation and decay of internal waves, wind-driven currents, microstructure, bottom boundary layer physics, equatorial currents,

*Dr. O'Brien is Program Director of Physical Oceanography at the Office of Naval Research. He is on leave from Florida State University where he is Professor of Oceanography and Meteorology.

western boundary currents and rings, mesoscale eddies, and mixed-layer dynamics. In addition, research in physical oceanography is required to understand the deep internal motions in the sea on a scale ranging from the general ocean circulation systems to small-scale turbulence and also the distribution and changes in physical properties of water masses, particularly as they concern ASW, ship routing, surface weather, forces on submerged structures, acoustic surveillance and weapons systems, deep-sea search and rescue, sea-bed inspection and assessment, and other naval operations.

In this issue of the *Naval Research Reviews* and in subsequent issues during the 30th birthday of ONR, several scientists will describe research aimed at meeting the program objectives. These papers will outline many of the advances made in understanding the ocean. Carl Wunsch reviews our knowledge of internal waves in the ocean. The structure of ocean fronts and their effect on sound velocity is described by Gunnar Roden. The utilization of fleet P-3 aircraft to monitor large scale temperature changes in the North Pacific is outlined by Tim Barnett. Ken Hunkins relates the problems of doing physical oceanography in the Arctic Ocean.

In other issues of the *Naval Research Reviews* this year, Bill Patzert writes on a study of El Nino, a massive fluctuation of the equatorial eastern Pacific Ocean which affects the major fisheries of Peru and Ecuador. Michael Gregg describes the detailed temperature profiles known as microstructure. Kristina Katsorus studies the smallest scale air-sea interaction in order to understand the momentum and heat transfer across the ocean surface. Phil Richardson and Andrew Vastano describe major Gulf Stream instabilities known as Gulf Stream rings. Numerical models of the ocean similar to atmospheric numerical weather prediction models will be commonplace when our data base for these models is sufficient. T. Laevastu and colleagues discuss an example.

Later this year another issue of *Naval Research Reviews* will describe the major field programs sponsored by the physical oceanography program: the North Pacific Experiment (NORPAX); POLYMODE, a major study of low frequency currents in the North Atlantic; the Indian Ocean Experiment (INDEX), a pilot study to prepare oceanographers to design experiments for 1979; and an ocean mixed layer experiment.

These twelve papers outline a substantial fraction of basic research being supported by ONR in physical oceanography. In reading the contributions, keep in mind that support for these programs is based on Navy relevance as emphasized by the Honorable J. William Middendorf II, Secretary of the Navy in his memorandum for the Chief of Naval Operations, dated 10 February 1976.

"The disciplines and programs supported by naval research should, in general, be those judged to be of greatest future potential for the needs of the Navy and Marine Corps. They should complement or strengthen the national research base in these areas. In the light of the Navy's particular or unique dependence on areas such as acoustic oceanography, our commitments to those disciplines should remain substantial."

Thermal Response of the Ocean to the Passage of a Typhoon

Highly significant changes in ocean temperature structure were observed to occur within less than one day when a Navy P-3 patrol aircraft took off from NAS Agana Guam on 14 Aug 1975 marking the start of Operation OSTroC 75. This operation, part of a project sponsored at the Naval Postgraduate School by the Office of Naval Research, was conceived to collect for the first time ocean thermal data immediately pefore and after the passage of a major tropical cyclone, such as a hurricane or typhoon.

Overall, project OSTroC is investigating aspects of the interactions between the Oceans and Severe Tropical Cyclones. The operation to collect ocean thermal data was planned and managed by CDR William Schramm, USN, a Ph.D. student in the Oceanography Department of NPS. The Seventh Fleet aircraft which conducted the flights were from VP-65, under the control of Fleet Air Wing One, Detachment Agana. Fleet Weather Central Guam helped coordinate the operation and provided the necessary data on the typhoon.

The first aircraft proceeded 680 NM northwest of Guam to an area of undistrubed ocean north of Typhoon Phyllis and dropped a pattern of SSQ-36 airborne expendable bathythermographs (AXBTs). The SSQ-36 measures the ocean temperature from the surface to 1000 ft. and transmits the information to the aircraft. These particular SSQ-36s had been calibrated by the National Oceanographic Instrumentation Center in San Diego in preparation for this operation. Within approximately 14 hours after the first flight, Typhoon Phyllis crossed the area with steady winds of 115 kts. gusting to 140 kts.

Just 10 hours after the eye of the typhoon had crossed the area of observation a second aircraft was on station dropping SSQ-36s. The points where data was taken on the first flight were revisited and also observations were taken along the typhoon track. The unique data from these flights represents the *first truly synoptic ocean data ever collected both before and after the passage of a major tropical cyclone*.

The third and final flight of the operation revisited the area 48 hours later and again observations were taken at the same points. The three flights took place over a period of 72 hours and covered a total of 8000 NM. Sixty-seven AXBT soundings were obtained.

Dramatic changes were observed under the path of the eye of the typhoon. The surface temperature decreased 3°F in 24 hours and the subsurface isotherms were moved upward on the order of 200 feet. This vertical motion or upwelling under the eye was observed down to 1000 feet.

Internal Waves in the Sea

Carl Wunsch*
Massachusetts Institute of Technology

Introduction

Internal waves, the waves occurring on the surfaces of density stratification, are a ubiquitous feature of the sea. Their theoretical study began in the nineteenth century, and they have been observed everywhere in the world oceans, from near the surface to the greatest depths that anyone has ever looked. At present, they are a field of very active research and progress for a great variety of reasons. They affect in sometimes profound ways, the propagation of sound through the ocean, and they are a major source of "noise" or contamination in any measurement of the mean properties of the ocean. But in addition, internal waves figure prominently in any discussion of the dynamical behavior of the ocean circulation. Internal waves may represent a major mechanism by which the ocean is mixed-maintaining the observed stratification, and generating the small scale "microstructure" of the oceans. It has been suggested (e.g. Muller, 1974) that they play a major role in dissipating the major currents of the oceans, and under some circumstances (Bretherton, 1969) they may be responsible for the reverse process: providing the driving mechanism for major current systems.

Because of these, and other effects, internal waves are currently being enthusiastically studied from a great many points of view. Here we will try to sketch some of the more interesting aspects of this work.

The study of internal waves is more difficult than of the more familiar surface waves. Not only is one faced with the problem of making measurements at great depth, but the wave periods are measured in hours rather than seconds, thus necessitating long duration measurements. Furthermore, the relationship between wavelength and frequency (the dispersion relation) is much more complex. If all this were not enough, internal waves undergo non-linear interactions much more readily than do surface waves.

Perhaps nor surprisingly then, the history of research on internal waves has been very different than for surface waves. Examining the relative state of knowledge is instructive since there are many analogous features of the two kinds of waves. Back in the very early pre-history

*Dr. Wunsch is a Professor in the Department of Earth and Planetary Sciences, Massachusetts Institute of Technology, Cambridge, Massachusetts. He has contributed to the basic understanding of ocean fluctuations, currents, and tides.

of man, someone realized that when the wind blew, waves were generated. Probably it was not much later that it was recognized that the longer the wind blew, and the further downwind one was, the larger the waves became. Perhaps it was even realized that with increasing wind and fetch, the waves grew in wavelength. In the eighteenth to twentieth centuries, dispersion relationships between period and wavelength (and later amplitude) were found. In the last two decades, research has provided understanding both of the detailed mechanisms by which the wind generates waves, and descriptions of the expected relation between wind speed, fetch, and wave amplitude as a function of frequency. This spectral description then relates the relative size and frequency of the waves to the forces generating them. Thus while our knowledge of the factors controlling all of the details of surface wave physics are by no means complete, there is in a qualitative sense excellent understanding of the relationships between generation, form, and propagation of the waves.

For internal waves, the history has been quite different. The dispersion relationships were worked out for the most part in the nineteenth century, but of course observation could not begin until the late nineteenth and early twentieth century with the invention of the reversing thermometer. In the past 5 years, Garrett and Munk (1972, 1975) produced a successful spectral description of internal waves.

This spectral description is a remarkable one in a number of ways. First, it was found that in quite distinct contrast to the case of surface waves, internal wave activity is essentially constant in space and time no matter where one looks (the very-near surface layers are probably an exception to this statement). That is, there is no analogy to periods of calm and of storm. Second, almost all observations are consistent with isotropic propagation; no analogy exists to the observed propagation of surface wave away from storm areas, particularly obvious in long trains of swell.

In the Garrett-Munk spectrum one has a remarkably good description of the internal wave field in the open sea. Indeed, the spectrum has stimulated a large number of experiments (see for example, Briscoe, 1975) in which it has been exceedingly difficult to find deviations from the Garrett-Munk spectrum. This is a very pleasant situation, for it means that one can go to almost any region of the ocean, and know in advance very nearly what the state of the internal wave field will be.

But it also leads to some interesting difficulties. The reason surface waves are directional, i.e. not isotropic, is that they carry energy from source regions (storms) to sink regions (often coasts). We recently pointed out (Wunsch, 1975) that the apparent description of internal waves as having isotropic, universal spectra implies that they have no sources or sinks. Herein lies the problem. The overall utility of the universal isotropic description of internal waves can hardly be doubted. But where do internal waves come from? Where do they go, i.e. where does their energy dissipate? Like surface waves we have a knowledge of the dispersion relations, and an excellent spectral description. But in distinct contrast to surface waves the one thing we still cannot identify is the source (or sources).

Before proceeding to examine the possibilities for sources, we need to take a closer look at the spectral description. Let f be the local Coriolis parameter (i.e. the frequency corresponding to the 1/2 period of a Foucalt pendulum at any given latitude), and let $\rho_0(z)$ be the mean density of the ocean, where z is the vertical coordinate. From ρ_0 and gravity, we can form the buoyancy frequency

$$N(z) = \left(\frac{-g}{\rho_0} \ \frac{\partial \rho_0}{\partial z}\right)^{1/2}$$

Then at any given location, internal waves can exist only in the band of frequencies (J)

$$f \leqslant \sigma \leqslant N$$

except very near the equator, where the lower limit has to be expressed in a more complex form. Thus the frequency spectrum of internal waves would be expected to lie in a band of periods ranging from about a day to a few minutes. A not un-typical spectrum of horizontal velocity from the ocean is shown in Figure 1. In the figure there is a distinct peak at the low frequency end, i.e. near f. These are the so-called inertial oscillations and are internal waves at the limiting frequency. The spectrum is seen to decay roughly as σ^{-2} away from the inertial peak, toward the high frequency cut-off. The statement of universality is that the quantity

$$E'(\sigma, \underline{k}) = E(\sigma, \underline{k}) | \ N(z)$$

is a universal curve, where E is the frequency wave-number spectrum, and that E depends only upon $|\underline{k}|$ the magnitude, and not the direction of the horizontal wavenumber. Figure 1 shows only a quantity related to

$$\int_{-\infty}^{\infty} \int_{-\infty}^{\infty} E(\sigma, \underline{k}) \, d\underline{k}$$

It is also clear from Figure 1 that the internal wave field does not exist in a vacuum, but is embedded in a field of low frequency energy that is more energetic than the waves themselves, and that there is a weak higher frequency continuum. Both these regions must be kept in mind as we further examine internal waves.

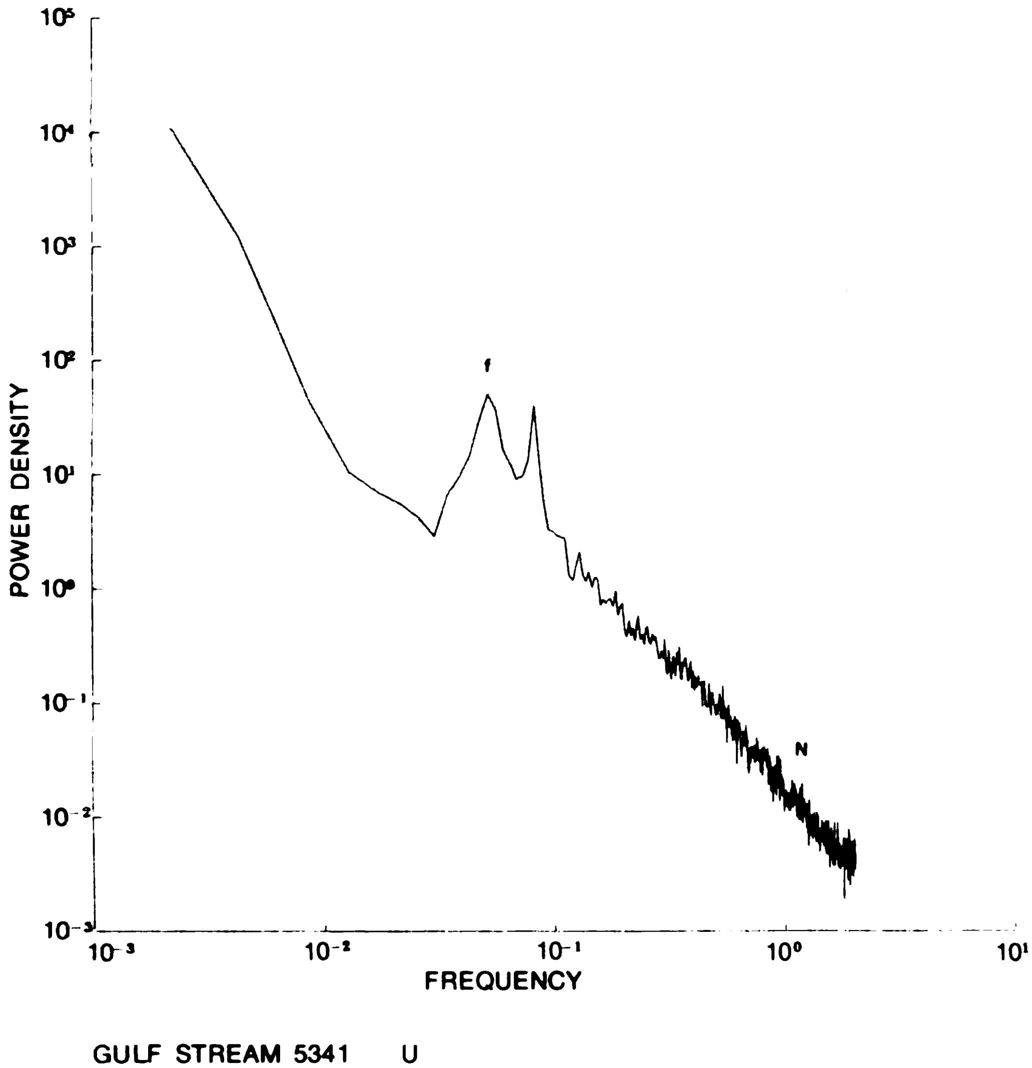

Figure 1 — Energy density spectrum of horizontal kinetic energy from a current meter at 3000 m depth. The frequency labelled f is the local inertial frequency, and N is the local buoyancy frequency. Most such records give similar spectra.

The Source and Sink Problem

Much current research is directed toward understanding the question of where internal waves come from. Theory (cf. Thorpe, 1975) suggests a number of possibilities: meteorological forcing, non-linear interaction with surface waves (energy extracted from surface waves and put into internal waves), the flow of currents including tidal currents over topography, and the large energy reservoir represented by the mean shear of strong current systems such as the Gulf Stream. None of these possibilities, and there are others too, has been actually demonstrated to be a source of internal waves.

How could one tell? Returning to the surface wave analogy, even if one has no sophisticated instrumentation, one deduces that they are generated by the wind, since high winds are usually associated with high waves. A man in a rowboat can tell that with an off-shore wind waves grow with fetch, thus introducing another obvious physical variable into the equation. Proceeding by analogy, one might then seek regions where internal waves are "highest" and see if such regions can be found, and whether they are associated with some common physical mechanisms. But merely finding such regions would not prove that a source region has been located. For surface waves are large in the surf-zone, a region where they are being dissipated. But simple physical reasoning allows one to distinguish between high energy regions that are sources and those that are sinks.

Recently, we have been attempting to locate regions where the internal wave field is more intense, or at least different, than normal. This effort has become feasible recently with the development within the Woods Hole Oceanographic Institution Buoy Group of stable mooring systems, allowing one to ignore problems of mooring motion contamination and other spurious effects. Given the success of the Garrett-Munk models however, one expects the search to be very difficult.

A determined search (reported in Wunsch, 1976) of Woods Hole and MIT data did turn up some suggestive physics. First, it was re-confirmed that the notion of a universal spectrum is a remarkably good one. Though the records came from very diverse parts of the north Atlantic, the great majority of the records are characterized by an essentially constant internal wave field. Astonishingly, the effects of the enormous currents and shear of the Gulf Stream region (the low frequency continuum) are barely noticeable, and may not even be real. An example of the distribution is shown in Figure 2.

The only clear inhomogeneity located anywhere in the deep western Atlantic was associated with Muir Seamount (Figure 3) a massive feature rising from 4800 m to 1600 m. Records made on and near this seamount show internal wave energies nearly an order of magnitude greater than in any other location yet found. The detailed energy distribution is shown in Figure 3. A spectrum of one of the higher energy records is shown in Figure 4. Since theory implies that bottom topographic features might be internal wave sources, (and it is difficult to see how Muir seamount could be a sink) it appears that here we have finally located a strong source of internal waves in the deep sea.

But the Muir seamount observation also suggests that the recovery of the internal wave energy to a universal spectrum is very rapid. 1000 m above the measurements shown in Figure 2 and 10 km away at the same depth, the spectra are indistinguishable from the Garrett-Munk model.

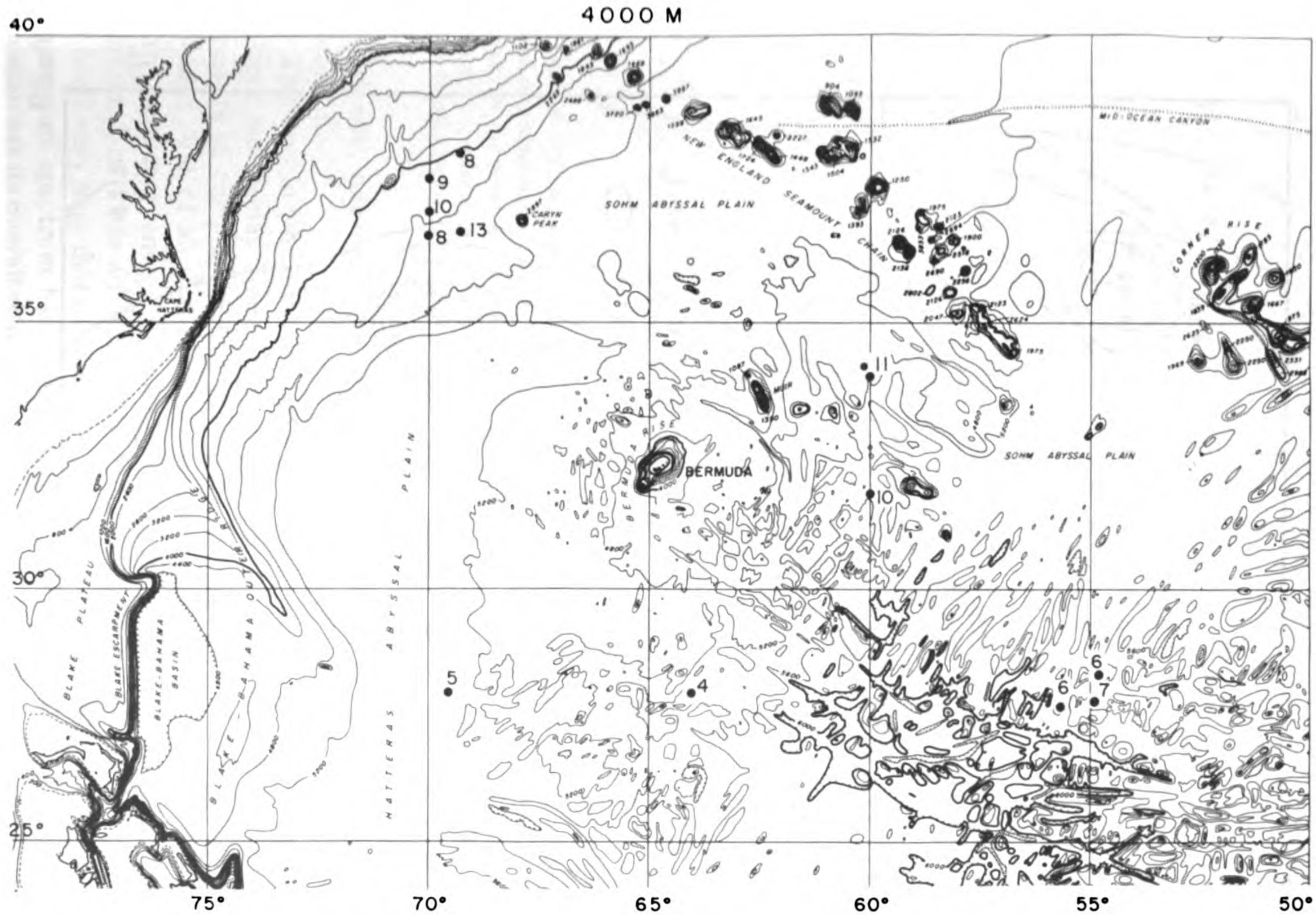

Figure 2 – Energy density, normalized by N(z), at 5 hours period in the western North Atlantic. The universal spectral model s predict a level of about 5. Chart adapted from one by E. Uchupi.

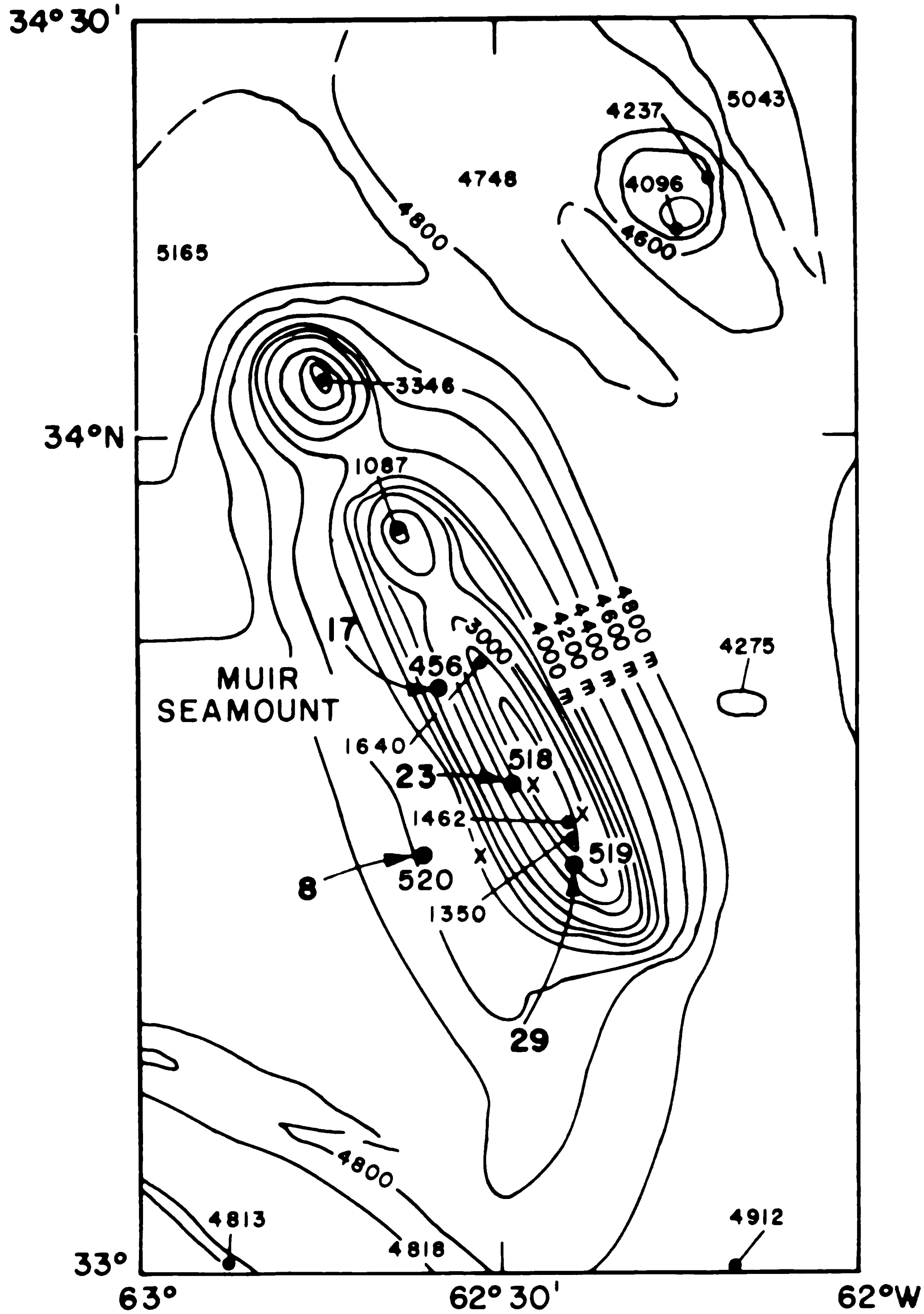

Figure 3 — Detail of the measurement made near Muir seamount, 518, 519, etc. are WHOI mooring numbers. Depth contours are in meters. Heavy numbers are normalized internal wave energy at 5 hours period.

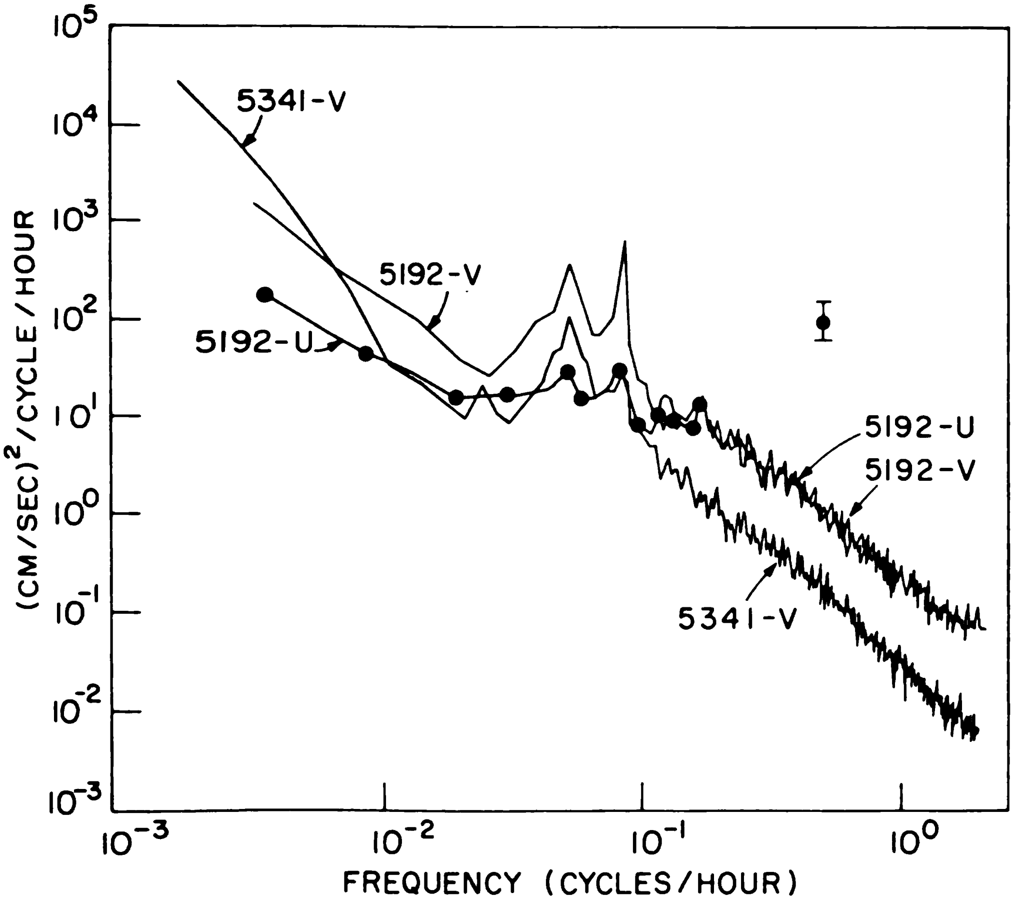

Figure 4 — Comparative power density spectra of a record obtained on Muir seamount and one obtained in the Gulf Stream region. The Gulf Stream region record (5341) is close to the level of the universal spectral models, but the Muir seamount record has nearly an order of magnitude more energy. Notice however the vastly greater energy at low frequencies in the Gulf Stream record.

Evidently, one must be virtually on top of a source before one can detect it.

The way in which the recovery must take place is shown in Figure 4. There we display kinetic energy spectra of one of the Muir seamount records in comparison to a record taken from the Gulf Stream region. Notice first of all that the Gult Stream region record has much more low frequency energy (by two-orders of magnitude) than near the seamount, but it has an order of magnitude less internal wave energy - at a level very near that required by the Garrett-Munk spectrum. The Muir seamount spectrum has nearly 10 times the energy of the equilibrium model, yet its overall shape is nearly the same. Whatever process controls the shape of the spectrum of internal waves must act extremely rapidly, and as we have already noticed, whatever controls its amplitude must act not very much more slowly.

Notice also that in Figure 4, the two components of velocity u(east) and v(north) have very different amplitudes near the low frequency cut-off. The inertial oscillation itself lies principally in the v component. In this part of the spectrum at least - there is a considerable degree of anisotropy - evidently a necessary condition for a region to be a source. Unfortunately one of our major lacks is actual measurements of the flux of energy away from the seamount. The experiment from which these measurements were taken was designed for quite a different purpose (see Hendry, 1975) and direct calculations of the energy derived from the seamount are not possible. Future experiments should be able to confirm or refute the notion that this large scale topographic feature is an internal wave source.

The Sink Problem

The problem of where internal wave energy is given up is in some ways more interesting than the question of where it comes from. For if there are regions into which internal waves pump a great deal of energy, one has possibilities for directly driving mean circulations. But here again, speculation has far out-run direct observations. Much surface wave energy is dissipated at beaches, and it is well known (e.g. Bowen, 1969) that incoming wave momentum may drive long-shore currents, rip-currents, etc. Similar processes have been hypothesized (Wunsch, 1971, Hogg, 1971) for internal waves and there is some evidence for the process in nature (Emery and Gunnerson, 1973).

If internal waves simply mix up the ocean in certain regions, e.g. over beaches, then mean flows, microstructure, etc. will be generated. A clear laboratory example of the breakdown and mixing of internal waves is given by Cacchione and Wunsch (1974)(Figure 5). From all of these pieces of evidence one expects very active regions of dissipation on slope regions and in related geographical areas, such as canyons. In particular, Shepard, *et al.*, 1974 have shown that very strong currents probably associated with internal waves are found in off-shore canyons. We cannot yet be sure how much internal wave energy is lost there, however.

Another possibility, under active investigation (e.g. Garrett and Munk, 1972b) is that the internal wave field is essentially self-dissipating, everywhere locally. By that is meant that much like surface waves, every once in a while a critical superposition of wave trains occurs making the waves locally so steep that they break -an analogue to the intermittent white-capping seen at the surface. At least two-processes have been suggested for the mechanism by which the waves break - a shearing instability (Kelvin-Helmholtz type) and a buoyancy instability (analogous to a toppling breaker). But examination of the details of such processes

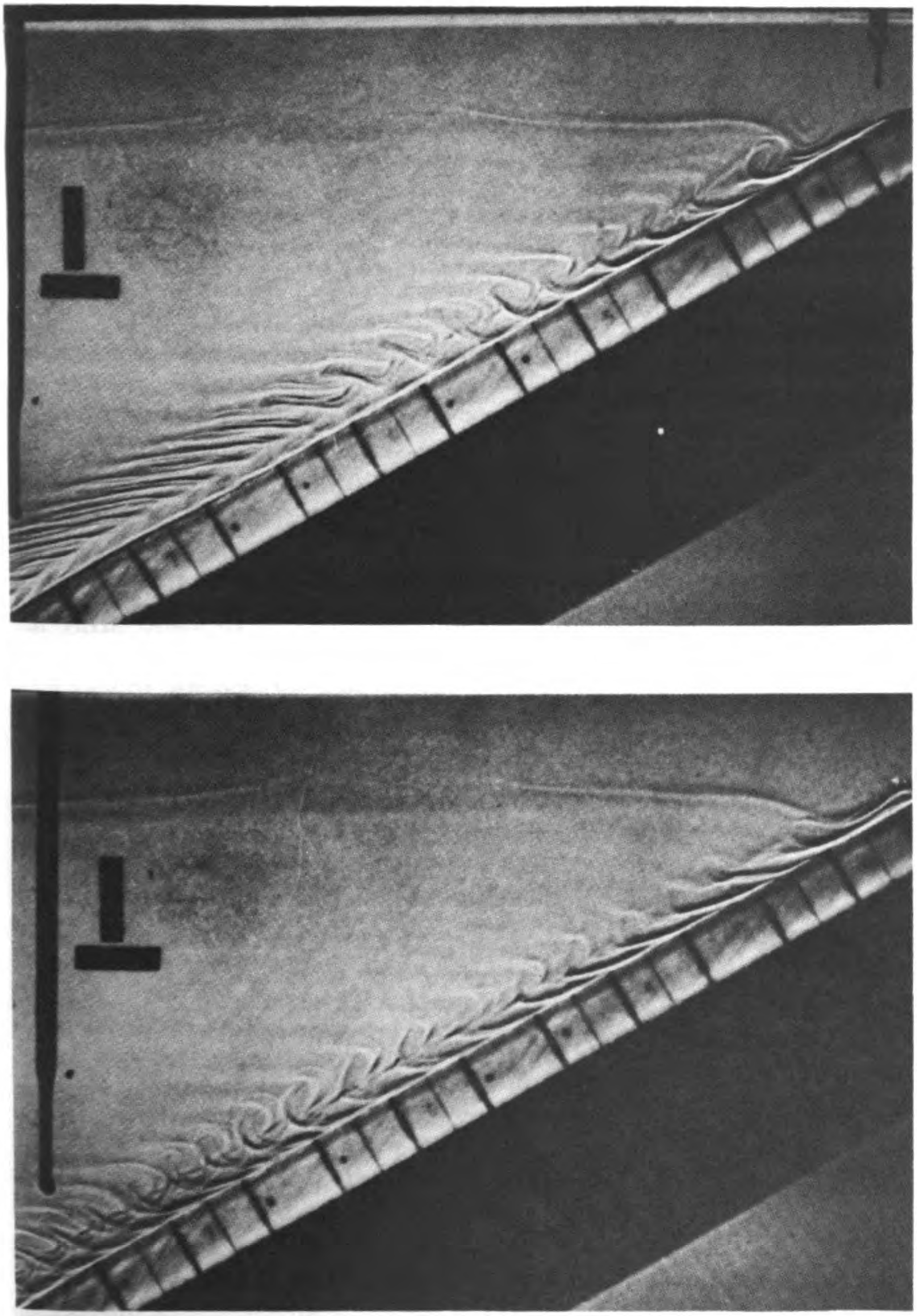

Figure 5 — Shadowgraph taken from Cacchione and Wunsch (1974) showing internal wave breakdown over a sloping region. Notice the generation of microstructure and the formation of a "borelike" phenomenon at the head of the advancing wave.

is difficult experimentally and theoretically, and our knowledge of the rates of breakdown, and the degree to which the ocean is thus mixed unknown.

One can begin to see in detail the breakdown of the internal wave field with certain special kinds of instrumentation. Small-scale mixing of the internal wave field may generate much of what has become known as the fine-or micro-structure that appears on density gradients in the sea. Many mechanisms have been proposed to generate and maintain this microstructure against the smoothing effects of diffusion. A leading contender is the internal wave field, but the processes of instability alluded to above must occur at spatial scales measured in meters horizontally and vertically. These are the scales that are usually inaccessible to our instrumentation - particularly in the horizontal.

In order to begin to measure these small horizontal and vertical scales, we have constructed a special "micro-scale array" for deployment in the main thermocline that measures over 20 m horizontally, and a few meters vertically, the 3 components of velocity, and temperature. The instrument (described by Eriksen, 1976) is a complex one, since to obtain the required precision means that orientation and motion of the instrument itself must be carefully monitored. The micro-scale array has yielded much useful information about small scales in the ocean, but perhaps the most graphic form of display can be seen in Figure 6. It shows the temperature over 8 m in the vertical as a function of time. The bulk of the up-and-down motion represents high frequency internal waves sweeping past the temperature sensors. But there is a period, preceded by a strong flow as measured on the current sensors, in which the water shows almost no stratification - indeed the closed isotherms show unstable stratification. Locally the fluid has become mixed - presumably by the internal wave field itself. A sensor lowered through this region would detect an inversion - or temperature fine-structure.

Thus there is good evidence here and elsewhere (see for example Cairns, 1975) that the internal wave field is at least partially responsible for mixing the ocean. Mixing processes however are probably the least understood of any oceanographic phenomenon. Much remains to be done in understanding the significance of events such as the one shown in Figure 6. Ultimately, one needs to be able to relate the existence of internal waves to quantitative parametric statements of the existence and intensity of such mixing events -converting them to simple mixing coefficients. There is a long-way to go.

The Spectral Shape

This is a fascinating question - why is the spectrum so nearly universal? We have already alluded to one possibility - that the spectrum is self-limiting. That is, if the internal wave energy increases beyond a critical

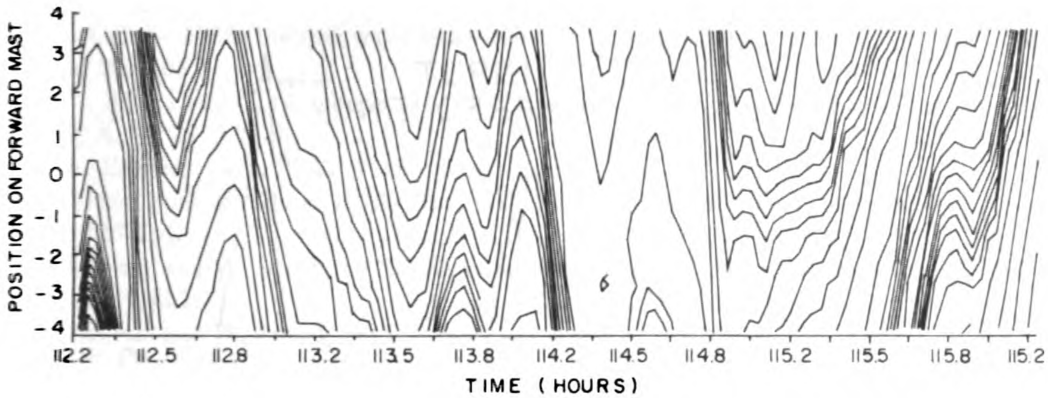

Figure 6 — Contours of temperature against time over an 8 meter vertical distance taken from Eriksen (1976). Rapidly changing contours are internal waves sweeping past the sensors. Notice mixed region with closed temperature contours showing breakdown of the mean stratification.

amplitude at a particular frequency, the waves will somehow break, removing energy and reducing the spectrum to a sup-critical level. At the present time, it is not known which criteria to apply to this process.

Another interesting possibility is that the non-linear interactions that internal waves are known to undergo operate in such a way as to export energy from one region of the spectrum to another in just such a way that a universal spectrum is maintained. An example of this type of interaction is shown in Figure 7 taken from Martin *et al.* (1972). In that experiment energy was placed via a paddle into a stratified wave tank at frequency σ_0. The wave is unstable and rapidly gives up energy to two additional waves at frequencies σ_1 and σ_2; such that $\sigma_0 \pm \sigma_1 \pm \sigma_2 = 0$. These waves are in turn unstable. Eventually one anticipates, that if the paddle were kept going long enough, and that if the tank were large enough, that something approaching a continuum of frequencies would result. A similar process is believed to occur in the ocean, but in the evident steady state observed, energy must be replaced at each frequency at the same rate that it is exported. Given a spectrum, one can in principal calculate the way in which that spectrum would change in time through resonant interaction. This calculation is quite difficult in practice, but has been carried out by Olbers (1974) for the Garrett-Munk model. He finds that energy, should be removed from intermediate frequencies and fed toward the inertial frequency.

Given Olbers' result, there are several possible conclusions. Either the Garrett-Munk spectrum is not a perfect description of the internal wave field, or the sources and sinks of internal wave motion are just such as to compensate the changes in time that Olbers' finds, or some other mechanism for controlling the spectral amplitude and shape is at work. All of these possibilities are under active investigation.

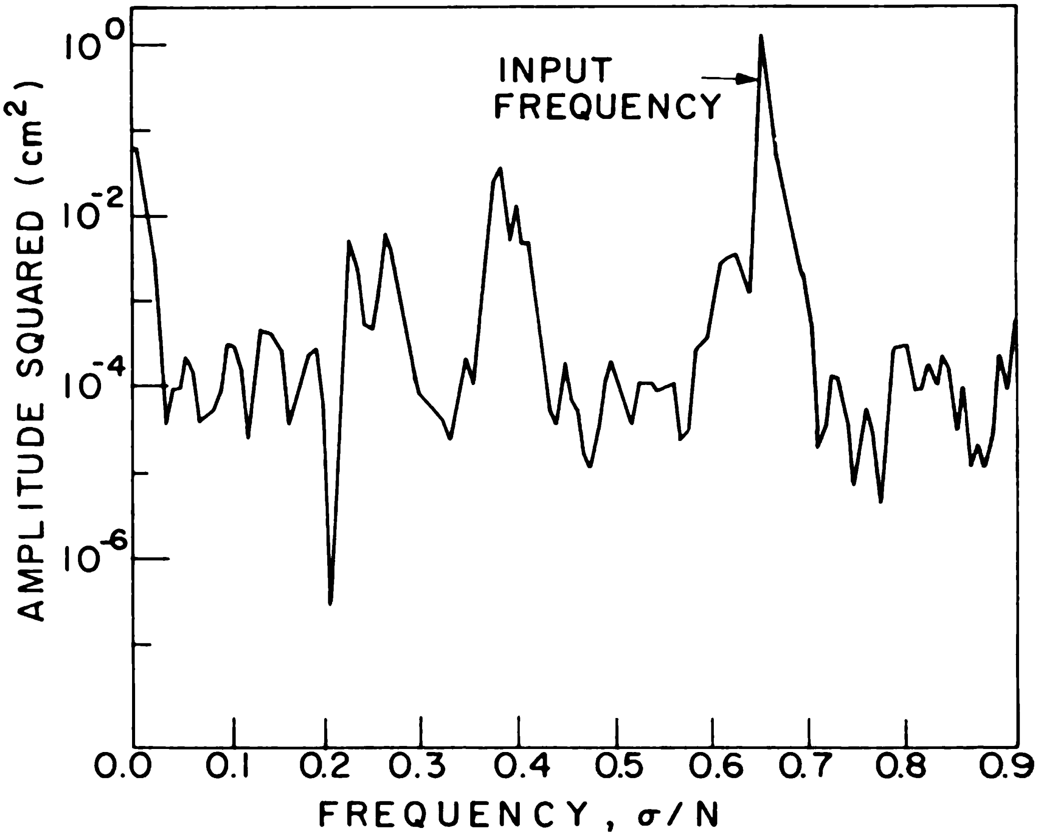

Figure 7 — Results of an experiment reported by Martin, et al. (1972). Energy was placed in a density stratified wave tank at the frequency indicated. Through resonant instability, energy appears at quite distinct frequencies far-removed from the frequency of input.

The birth, life, and death cycle of internal waves is thus very intimately linked to the dynamics controlling the entire structure and motion of the overall ocean circulation. One of the fascinations of the subject is the way in which highly disparate motions, on different time and space scales, may interact to produce unexpected interconnections. The internal wave field will only be fully understood when most aspects of the general circulation are understood.

References

A. J. Bowen, 1969, The generation of longshore currents on a plane beach, J. Mar. Res., **27**, 206-225.

M. G. Briscoe, 1975, Preliminary results from the tri-moored internal wave experiment (IWEX), J. Geophys. Res., **80**, 3872-3884.

F. P. Bretherton, 1969, Momentum transfer by gravity waves, Quat. J. Roy. Met. Soc., **95**, 213-243.

D. A. Cacchione and C. Wunsch, 1974, Experimental study of internal waves over a slope, J. Fluid, Mech., **66**, 223-239.

J. L. Cairns, 1975, Internal wave measurements from a mid-water float, J. Geophys. Res., **80**, 299-306.

K. O. Emery and C. G. Gunnerson, 1973, Internal swash and surf, Proc. Nat. Acad. Sci., USA, **70**, 2379-2380.

C. A. Eriksen, 1976, Ph.D. Thesis, in preparation.

C. Garrett and W. Munk, 1972a, Space-time scales of internal waves, Geophys. Fl. Dyn., **3**, 225-264.

C. Garrett and W. Munk, 1972b, Oceanic mixing by breaking internal waves, Deep-Sea Res., **19**, 823-832.

C. Garrett and W. Munk, 1975, Space-time scales of internal waves: A progress report, J. Geophys. Res., **80**, 291-297.

R. Hendry, 1975, The generation, energetics and propagation of internal tides in the western North Atlantic Ocean, Ph.D. Thesis, MIT/WHOI.

N. G. Hogg, 1971, Longshore current generation by obliquely incident internal waves, Geophys. Fl. Dyn., **2**, 361-376.

S. Martin, W. Simmons and C. Wunsch, 1972, The excitation of resonant triads by single internal waves, J. Fluid. Mech., **53**, 17-44.

P. Muller, 1974, On the interaction between short internal waves and larger scale motions in the ocean, Hamburger Geophysikalische Einzelschriften, Heft 23, 98.

D. J. Olbers, 1974, On the energy balance of small scale internal waves in the deep-sea, Hamburg Geophysikalische Einzelschriften, 24.

F. P. Shepard, N. F. Marshall and P. A. McLaughlin, 1974, "Internal waves" advancing along submarine canyons, Science, **183**, 195-198.

S. A. Thorpe, 1974, The excitation, dissipation and interaction of internal waves, J. Geophys. Res., **80**, 328-338.

C. Wunsch, 1975, Deep ocean internal waves: what do we really know? J. Geophys. Res., **80**, 339-343.

C. Wunsch, 1976, Geographical variability of the internal wave field: a search for sources and sinks, to be published.

C. Wunsch, 1971, Notes on some Reynolds stress effects of internal waves on slopes, Deep-Sea Res., **16**, 583-591.

Internal Rossby Waves Discovered in N. Pacific

The existence of internal (baroclinic) Rossby Waves in the ocean has not been firmly established. Dr's. Magaard and Emery, ONR Contractors at Hawaii, have recently shown that the month-to-month variation in temperature structure in the northeastern Pacific may be interpreted as internal Rossby waves. The dominant waves have wave periods of 7 to 28 months; they propagate westward at several centimeters per second; their wavelength is of the order of 1000 km long. The temperature variation in the upper ocean due to these waves changes the sound velocity regime. Inter-annual (i.e., several months) variations in sound velocity of a few meters per second is accounted for by these waves in the upper 500 m of the Pacific.

203-429 O - 76 - 3

On the Structure and Prediction of Oceanic Fronts

G. I. Roden*
University of Washington

Introduction

Frontal zones play an important part in ocean dynamics and energetics. They are regions of intensified motion, sharp gradients, decreased stability and increased turbulence and convection. Storms often form in regions of oceanic fronts, where the energy exchange between the sea and the atmosphere is vigorous. The long range sound transmission is strongly affected by the presence of fronts, and the thermal inversions, which often accompany them. The study of oceanic fronts is relevant, therefore, not only to the science of oceanography, but also to the sciences of meteorology and underwater communication.

Fronts are observed in every ocean, in surface as well as subsurface layers, and on scales varying from planetary to local. Many fronts occur in geographically preferred regions, determined by the planetary wind and current systems, the heat, salt and water exchange at the sea surface and by the bottom topography. Within these regions fronts are quite variable in time and move, intensify and decay in response to changing oceanic and atmospheric flow patterns.

At the sea surface, frontal regions are often marked by slicks, foamlines and aggregates of particulate matter, suggesting particle convergency. At times, there is a conspicuous change in water color, which can be attributed to the confluence of currents of different origin and biological productivity. Sometimes, distinctive acoustical noises are heard, where vigorous currents meet each other (1).

Oceanic fronts differ from the better known atmospheric fronts in several important ways. In the atmosphere, temperature and density fronts almost always coincide so that the frontal zones are highly baroclinic, with jet streams prominent in the higher elevations (2). In the ocean, no unique relation exists between the temperature and density fronts, because of varying salinity. If the temperature and salinity fronts point in the same direction, the density front is often weak or nonexistent, the baroclinity is small and there is no jet stream (3).

---

*Dr. Gunner I. Roden is a Senior Research Associate in the Department of Oceanography, University of Washington, Seattle. He has systematically mapped out the character and dynamics of the major ocean fronts in the North Pacific Ocean during the past several years.

Because of these fundamental differences, the study of oceanic fronts has to proceed along paths that differ from the classical atmospheric approach. Instead of regarding fronts as density discontinuities, it is necessary to define fronts as the maximum magnitude of a gradient a specific variable can attain. The relevant questions to ask are: "what processes lead to the intensification of the magnitude of a gradient?" and "how large can the magnitude of a gradient get?" The answers to the questions lead directly to the problem of frontal prediction.

To solve the problem of frontal prediction, it is necessary to regard the sea and the atmosphere as an interacting system, and to link the frontal structure and dynamics to the fluctuations of the major wind and current systems and to the energy exchange through the sea-air interface. In shallow water, the bottom topography and the configuration of the coast line have to be considered also (4).

At present, the state of research on oceanic fronts is in a stage of rapid development and it is important to summarize recent findings.

Thermohaline and Sound Velocity Structure of Oceanic Fronts

The study of frontal structure received strong impetus with the development of continuously recording electronic sensors, which could be lowered at frequent intervals across the frontal zone, or towed behind the ship. The instruments in common use today permit one to resolve vertical features of the order of meters and horizontal features of the order of kilometers. Closer horizontal resolution is possible with towed sensors, if the navigation is good.

Though the detailed thermohaline and sound velocity structure varies from one front to another, certain fundamental features are common. Most oceanic fronts occur in the upper kilometer of the ocean. The horizontal gradients are often strongest in or above the pycnocline. When the pycnocline is well developed, the upper part of the front can separate from the lower one under the influence of strong and persistent winds. The separation can reach 300 km, in some cases.

Temperature, salinity and density fronts in the upper layer need not occur at the same geographical location. This is a consequence of radiative heat transfer, evaporation and precipitation processes, which act independently of each other. Fronts below pycnocline depth are usually congruent, because the above named processes are insignificant or absent.

Not all oceanic fronts are baroclinic. Baroclinity is small, where horizontal temperature and salinity gradients tend to balance each other. The occurence of baroclinic jets is limited to unbalanced temperature and salinity fronts of substantial vertical extent. If these fronts are inclined with respect to the vertical, the jet axis will be some distance from the position of the surface front.

Internal fronts are sometimes observed, which have no surface manifestation. Such fronts result from differential vertical motion and are most often encountered near submarine ridges and where the curl of the wind stress changes rapidly.

The basic types of oceanic fronts are as follows:

a. Fronts Associated with Strong Boundary Currents. These are most pronounced at the poleward edge of the Kuroshio and the Gulf Stream and can be traced from the coast several hundred kilometers seaward (5). The fronts result from the intrusion of warm and high salinity water of subtropical origin into higher latitudes. The fronts are deep and highly baroclinic and in quasigeostrophic balance (6). The Kuroshio front at latitude 38°N, longitude 154°E, shown in Figure 1 is typical. The thermohaline and sound velocity gradients are well developed in the upper 300 m. The front is vertical in the upper 50 m and then slopes slightly to the southward. The core of the baroclinic jet is to the south

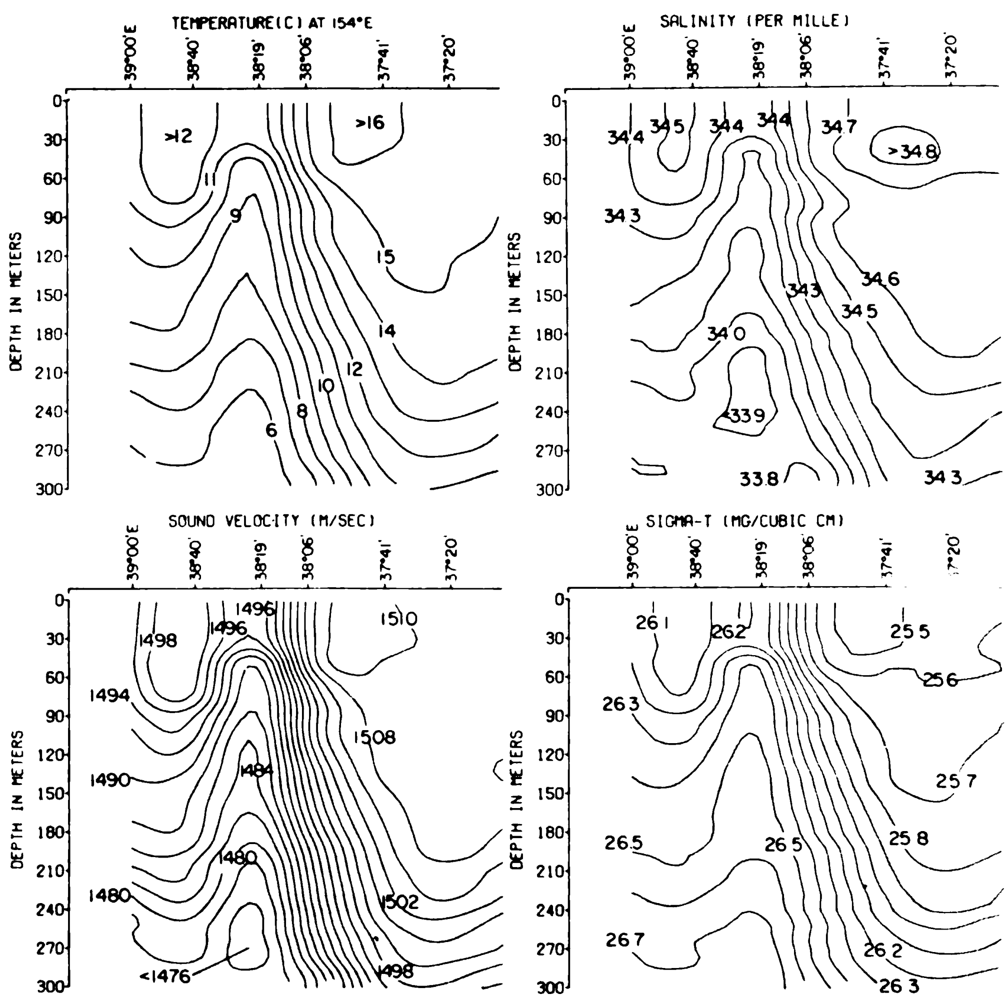

Figure 1 — Kuroshio front at longitude 154°E in April 1971

of the surface front, therefore. The Kuroshio and Gulf Stream fronts come closest to resembling the classical atmospheric fronts (2).

b. Fronts Associated with the Convergence of Ekman Transports. These are intimately related to the configuration of the wind stress field and occur in regions of strong positive wind stress shear. The subarctic front is often found to the south of the west wind maximum and the subtropical front occurs usually to the north of the easterly trade winds (7). The fronts are strongest in the surface layer.

The subarctic front at latitude 42°N, longitude 168°E is shown in Figure 2. It represents a boundary between the cold and low salinity subarctic water to the north and the warmer, higher salinity water of the central Pacific to the south. The subarctic front is most pronounced in the upper 120 m, where horizontal temperature gradients of 8°C/36 km, horizontal salinity gradients of 1.1%°/36 km, and horizontal sound velocity gradients of 28 m sec^{-1}/36 km are encountered. In contrast, horizontal

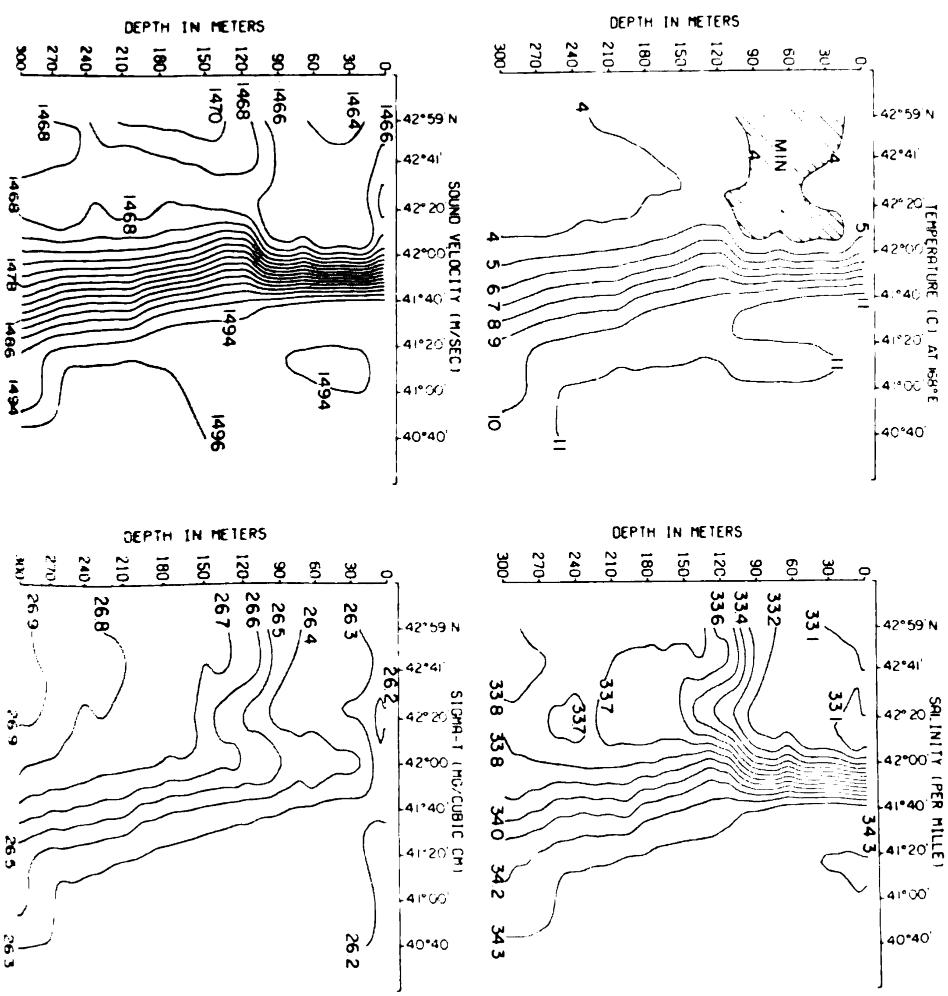

Figure 2 — Subarctic front at longitude 168°E in April 1971

density gradients in the top 120 m are small, indicating an almost complete balance between the horizontal temperature and salinity gradients. This lack of baroclinity in the upper layer distinguishes the subarctic front from the fronts associated with western boundary currents.

There is a marked change in water thermohaline structure across the subarctic front. North of the front, the distinguishing features are the temperature minimum and the thin high stability layer related to the halocline at 120 m. South of the front, there is no temperature minimum and no high stability layer. The lack of stability favors deep convection, as is seen by the isothermal and isohaline layers almost 300 m deep. The Sofar channel axis is strongly affected by the structural change at the front, descending from 50 m to more than 300 m over a distance 30 km (3).

The subtropical front of the Pacific is shown in Figure 3. It represents a boundary between the warm and high salinity subtropical water and the cooler and lower salinity water to the north. The outstanding feature is the separation of the upper part of the front from the lower one at the mean depth of the pycnocline. The surface front occurs at latitude 31°N, almost 300 km to the north of the subsurface front. Strong and persistent easterly winds had been blowing for a week when this section was taken, suggesting a northward displacement of the upper mixed layer by Ekman transport. The separation of the upper and lower parts of the front leads to the interesting fact that the strongest baroclinic flow is not found at the location of the surface front, but three degrees of latitude to the southward (7).

The subtropical front varies with season. The surface salinity front is present throughout the year, but the surface temperature and sound velocity fronts disappear during the summer months due to strong and uniform heating. Below pycnocline depth, the fronts persist through all seasons.

c. Fronts Associated with the Convergence of Surface Energy Fluxes. These fronts depend strongly upon the configuration of the surface heat and salt flux fields and occur often at cloud cover, precipitation and wind boundaries. The fronts are quite shallow, usually not exceeding 50 m. Because the surface heat and salt fluxes act independent of each other, temperature and salinity fronts do not coexist. A typical example is the doldrum front at latitude 11°N, longitude 133°W, which occurs at the transition from the rainy doldrums to the drier trade wind region The doldrum front is essentially a salinity front, which is not balanced by a temperature front. The imbalance gives rise to strong baroclinity in the surface layer, favoring an eastward current. The doldrum boundaries are one of the few oceanic regions where baroclinity is created exclusively by the salinity field (8).

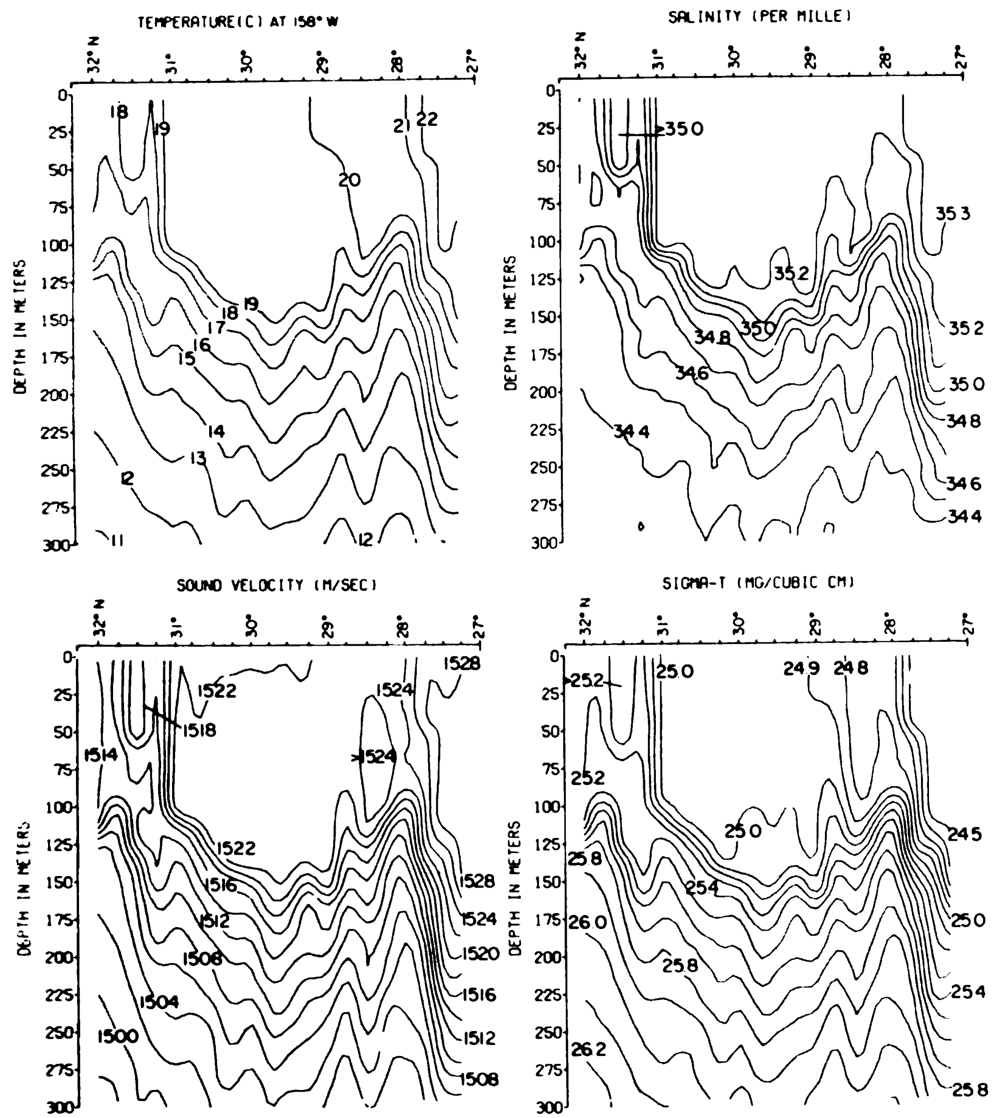

Figure 3 — Subtropical front at longitude 158°W in January 1975

d. Multiple Fronts Attributed to Baroclinic Rossby Waves. **Regularly spaced temperature, salinity and sound velocity fronts have been observed off northeastern Japan for several hundred kilometers seaward (7). These fronts are very strong in the upper 150 m and are spaced at intervals of about 70 km (Figure 4). Horizontal temperature gradients of 9°C/30 km, horizontal salinity gradients of 1.5‰/30 km and horizontal sound velocity gradients of 30 m sec^{-1}/30 km are observed here. The observed spacing of the fronts is close to the cutoff length of the baroclinic Rossby waves in a two-layer ocean (9), which have been implicated in instability generation (10). The subject of multiple fronts has not been investigated thoroughly to date and much further research is needed, before definite conclusions can be drawn.**

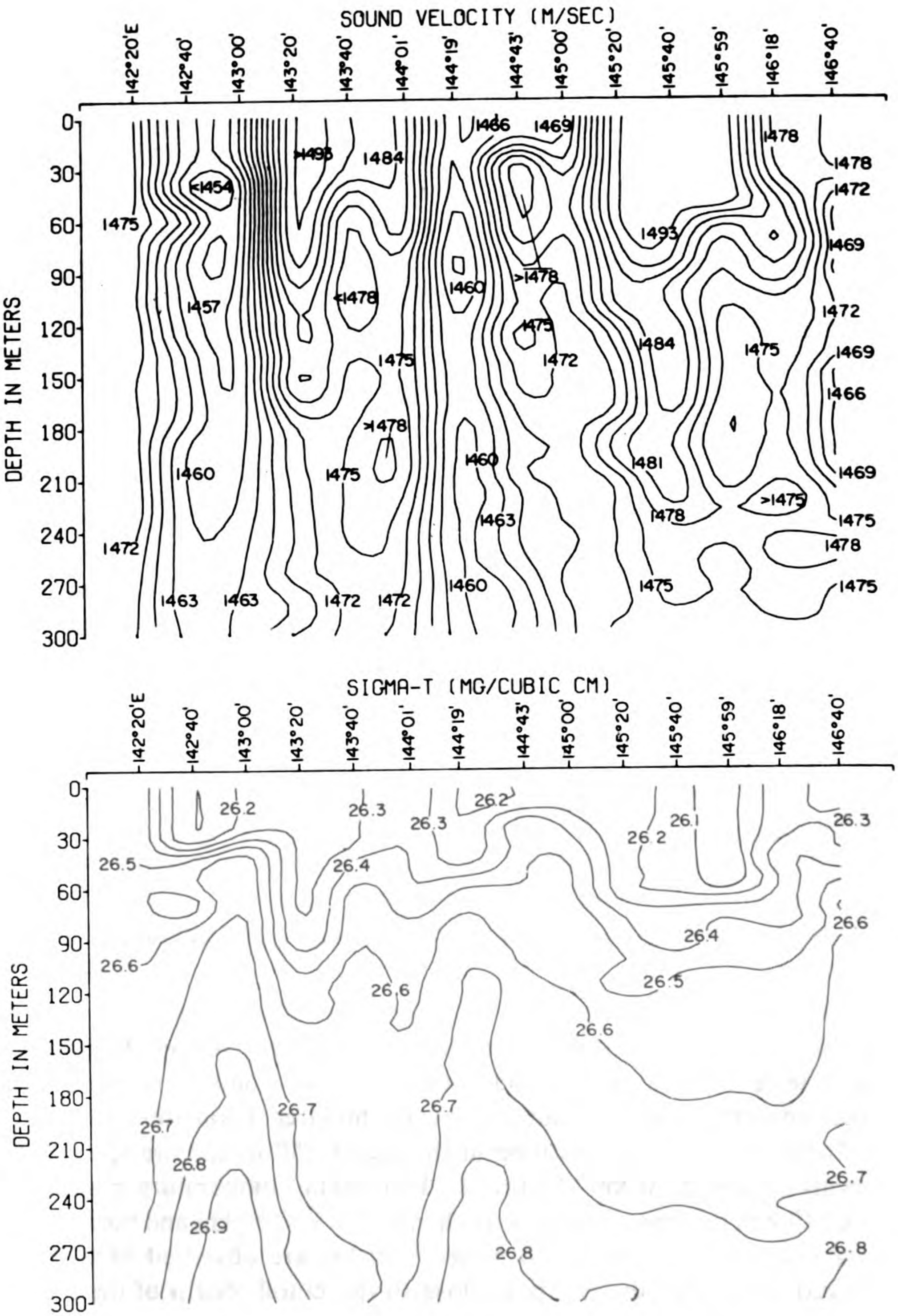

Figure 4 — Multiple sound velocity and density fronts at latitude 40°N off northeastern Japan.

The Shape of Thermohaline and Sound Velocity Fronts

Frontal zones are not uniform, but consist of intermittent regions of strong and weak gradients and have a tendency to meander. Though these features were recognized almost a century ago (1), only recently has the technology advanced to such a degree that meaningful large scale studies can be made. The recent advances are largely due to the development of modern radiative transfer theory and the use of satellite imagery. Strong surface temperature fronts are determined by contrasts in infrared radiation. The results are good, where the skies are cloudless or only partly covered by clouds. Both upwelling fronts (11) and Gulf Stream fronts (12) have been investigated by this means. The results show the presence of eddies and numerous meanders. Satellite observations have been used also to study current boundaries by methods of specular optics and color contrasts (13). The former depends on differences in sea state and the latter is based on differences in particulate matter. Both methods have been employed, with some success, in coastal regions and along the north wall of the Gulf Stream (13). It is interesting to point out that the infrared, specular optics and color methods are independent of each other and are capable of distinguishing fronts of different origin. The use of satellites in frontal analysis is just beginning and is promising, however, only surface fronts can be studied by this method.

Statistical determination of the shapes and meanders of fronts is still in its infancy and no unified conclusions can be drawn. A few preliminary statements on shapes can be made, however, based on past work (1, 5, 7).

In the upper mixed layer, where nonconservative processes such as radiative heat transfer and salt flux due to evaporation and precipitation are important, the shape of the temperature front may differ considerably from that of the salinity front. Where the temperature and salinity fronts are separate, a density front will accompany each of them, but where they overlap, a density front may, or may not occur, depending upon the degree of thermohaline balance. Therefore, the shape of the density front may differ from the shapes of both temperature and salinity fronts.

At depths below the upper mixed layer, the shapes of temperature, salinity and sound velocity fronts are usually identical, because of the absence of significant nonconservative processes. The existence of a similarly shaped density front can be inferred from the above only, if the thermal and haline fronts do not balance each other.

At strongly baroclinic fronts, the configuration of the jet axis is similar to the shape of the thermohaline front, but the two need not coincide at the sea surface. This is particularly true when the thermohaline front slopes with depth.

Fronts in Relation to Atmospheric Forcing Functions

Frontogenesis in the upper ocean is strongly dependent upon the momentum, heat and salt flux fields at the sea surface. These fields change with time, and it is of interest to look at the seasonal as well as non-seasonal variations. In mid-ocean, where the baroclinic flow is weak, regions of temperature and sound velocity frontogenesis can be delineated from the configuration of the wind stress field, which determines the field of Ekman mass transports in the upper layer, and from the configuration of the surface radiative heat flux field. Frontogenesis will reach a maximum, where strong Ekman transport convergence occurs in a region of radiative flux convergence.

The seasonal variation of the surface Ekman transports is shown in Figure 5, where the arrows indicate the direction of transport. The figure is based on northern hemisphere sea level atmospheric pressure maps, from which the stress of the geostrophic wind and the resulting transports were obtained for a one degree latitude-longitude grid (7). The seasonal

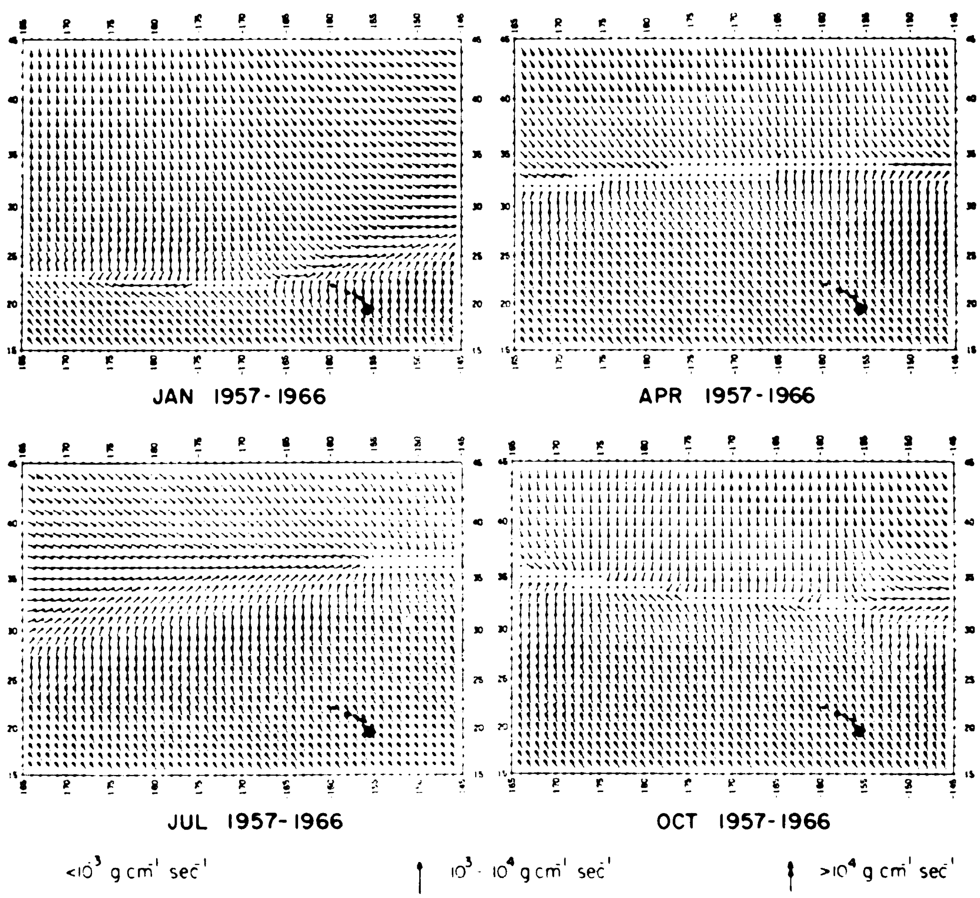

Figure 5 — Long term season variation of surface Ekman mass transport based on a one degree latitude longitude grid. Arrows indicate direction of flow.

variation of the Ekman transport confluence zone is clearly indicated. During winter, this zone lies between latitudes 23 and 28°N, during summer it lies between 34 and 37°N and during spring and fall, it lies between 32 and 35°N. The orientation of the confluence zone is predominantly zonal, on a long term seasonal average.

The seasonal variation of the surface net radiative downward flux can be computed from on satellite cloud cover observations (14) and surface meteorological information, evaluated on a one-degree latitude longitude grid (8). During winter, meridional radiation gradients are fairly uniform. During spring and fall maximum gradients are encountered between 30 and 35°N. During summer, the zone of maximum gradients has shifted to the north of 35°N.

Maximum temperature and sound velocity frontogenesis can be expected to occur during the spring and fall months in the latitude range between 30 and 35°N, when the convergence zone of Ekman transports coincides with that of the meridional radiative heat fluxes. This has also been confirmed by numerous shipboard investigations of the subtropical temperature front (7, 8) as well as by satellite studies (Bernstein, personal communication).

The nonseasonal variation of surface Ekman transports is shown in Figure 6 for four weekly periods in the winter of 1974 (7). The outstanding feature is that the displacements of the convergence zone during one winter month are as large as the longterm seasonal displacements. The observed fronts (large dots) all occured near the convergence zone, indicating that upper ocean fronts adjust themselves quickly to changing atmospheric conditions.

Spectral Structure and Thermohaline Perturbations Near Fronts

In frontal regions, temperature and salinity profiles with depth show considerable fine structure. The fine structure can be studied by applying a smoothing filter to the vertical profiles and removing the mean. The resulting records show temperature and salinity perturbations with depth, which can be analyzed by spectral and bispectral methods (15, 16, 17). The thermohaline perturbations near the subarctic front of the central North Pacific are shown in Figure 7. The figure was obtained by applying a 41 point binomial filter to records originally sampled at 3 m intervals, in the upper 1500 m of the ocean. The outstanding feature is that large perturbations are confined to a limited depth interval, here between 200 and 600 m. In the uppermost layer of the sea mixing effectively eliminates small scale structural features. At great depths, the motion is sluggish and the thermohaline gradients are weak. Hence, a region of increased perturbations lies between the surface and deep layers. The vertical length scales of the perturbations can be determined

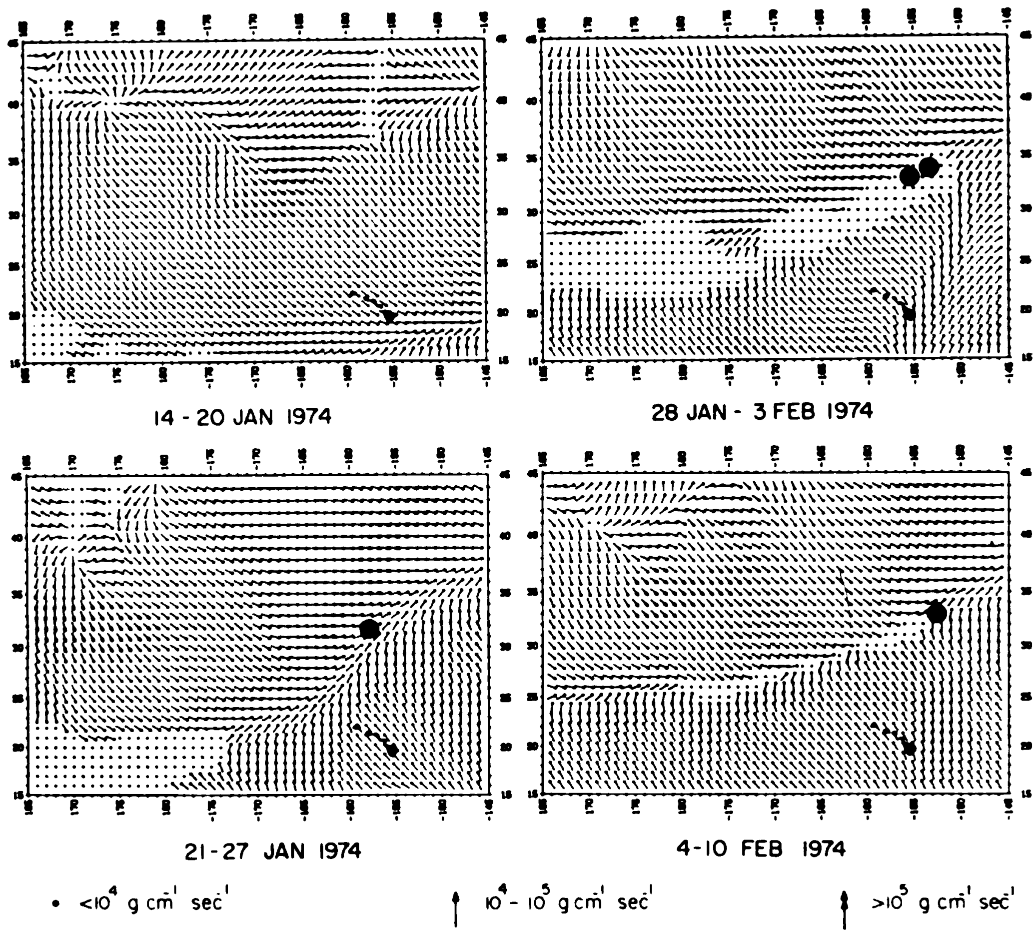

Figure 6 — Nonseasonal variation of the surface Ekman transport based on a one degree latitude-longitude grid. Arrows indicate direction of flow. Large dots indicate fronts observed during the R/V THOMAS G. THOMPSON cruise.

by methods of zero crossing analysis. In the central North Pacific, temperature and sound velocity perturbations are, on the average, 13-16 m thick, while salinity and density perturbations have a mean thickness of 8-10 m. The maximum perturbation amplitudes in this region are typically 0.2°C for temperature, 0.05% for salinity, 0.7 m sec^{-1} for sound velocity and 0.05 mg cm^{-3} for σ_t - density. In general, the vertical length scales and the perturbation amplitudes vary from one front to another. The largest amplitudes are observed off northeastern Japan, at the confluence of the Kuroshio and Oyashio currents, where the perturbations are ten times larger than at the subarctic front of the central Pacific (16).

a. Observed Wavenumber Spectra with Respect to Depth. It is of interest to look briefly at the information that can be obtained from the power spectrum determined over the 0-1500 m depth interval. The pertinent questions to be asked are: 1) How does the spectral density decrease with increasing wavenumber? 2) Are there any preferred wavenumbers at which the spectral density is concentrated? 3) For the same

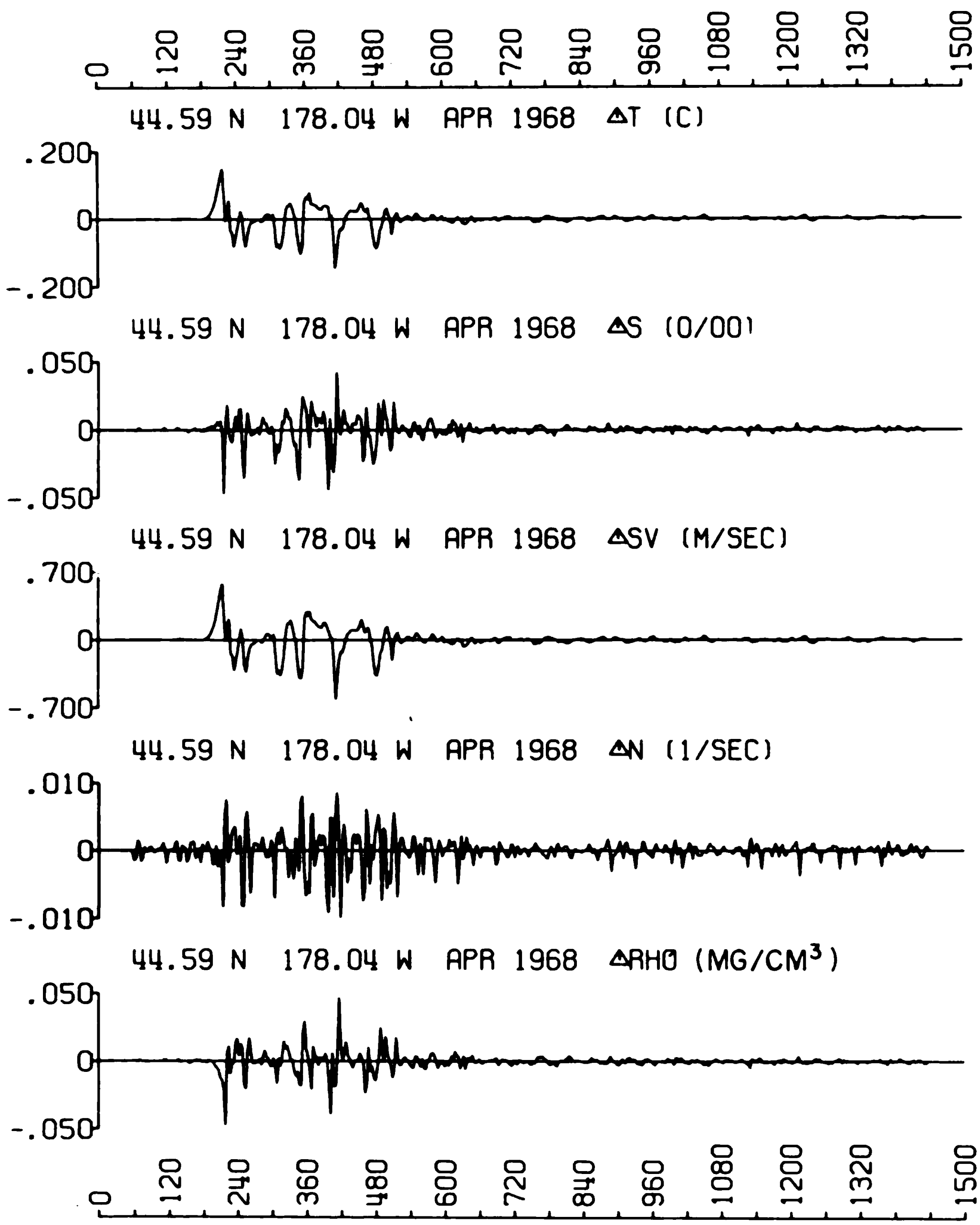

Figure 7 — Perturbations from the mean as a function of depth (m), obtained by binomial filtering: T, temperature; S, salinity; SV, sound velocity, N, Vaisala frequency; RHO, density.

variable, does the shape of the spectrum depend on geographical location? 4) For different variables at the same station, are the spectral shapes the same?

The power density spectra vertical temperature perturbations are shown in Figure 8. The computations were carried out for the wavenumber range between 0 and 167 cycles per kilometer (c.p. km) with a resolution of 3.33 c.p.km. All spectra were corrected for binomial filtering and plotted on a log-log scale. In each case, the number of data points was 501, and the degrees of freedom were 23.5. The inset scales refer to the 95% confidence limits.

The power density of the temperature perturbations decreases with increasing wavenumber, rapidly at first and then more slowly. The decay coefficient is not constant, but declines from -8/3 at low wavenumbers to about -6/3 at higher wavenumbers. The range of wavenumbers is in agreement with both turbulence in a stratified medium (14) and wave motion in a strongly layered fluid (15). The former theory predicts decay coefficients between -9/3 and -5/3 in the buoyancy - inertial subrange, while the latter requires a decay coefficient of -6/3.

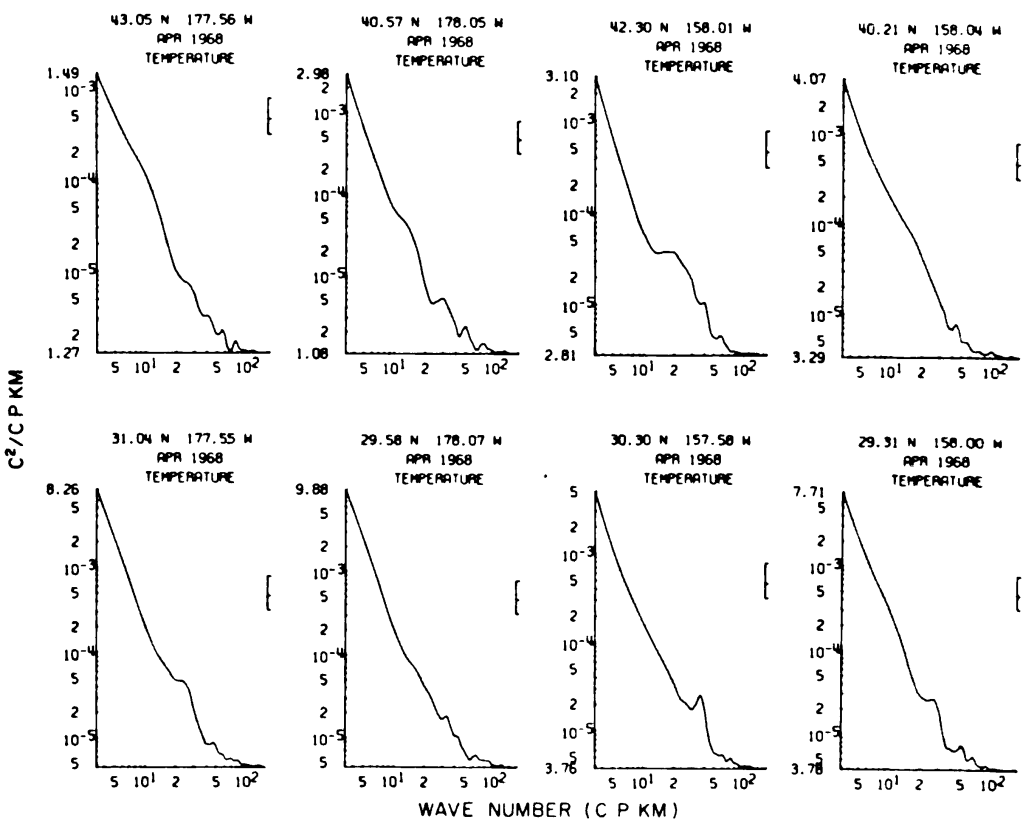

Figure 8 — Wavenumber spectra of temperature perturbations. Arrows indicate 95% confidence limits.

The observational evidence at present is not good enough to distinguish between these mechanisms. There are several small peaks in the temperature spectra, none of them significant at the 95% confidence level. It is noteworthy that the shape of the temperature spectra does not differ greatly at the subarctic and suptropical fronts of the Pacific, suggesting that the physical processes leading to the perturbations are similar at the open ocean fronts.

The power spectra of salinity are similar to those of temperature at low wavenumbers, with decay coefficients varying between -9/3 and -8/3. As the wavenumber increases, the decay coefficient decreases, but its exact value at higher wavenumbers is difficult to obtain, because of superimposed random fluctuations. A few significant peaks occur in the wavenumber range between 60 and 80 c.p.km, suggesting the existence of preferred vertical length scales of 13-17 m, at some stations. The reasons for the existence of such prefered length scales and their geographically intermittent character is not well understood at present.

The power spectra of sound velocity perturbations resemble those of temperature perturbations, while the power spectra of density perturbations are similar to those of salinity perturbations (15). At low wavenumbers, their shape is almost identical and independent of geographical position.

b. Observed Wavenumber Bispectra with Respect to Depth. The use of ordinary spectra for extracting information has basic limitations (18). From the turbulence point of view it assumes that the processes are fully described by second order correlation functions, such as in the Gaussian case. From the point of wave theory, it assumes that the observations consist of linear superposition of independent individual wavelets of random phase, such that the wavelets can pass through each other without distorting amplitude or wavenumber. In the real ocean, conditions for isotropy rarely exist in frontal regions, because of horizontal and vertical stratifications and the presence of currents. Third and higher order correlation functions are then required to describe the process. Third order correlation functions, and their Fourier transforms, called bispectra, are also required in a study of wave interactions.

The interpretation of bispectra centers on determining the slopes and shapes of bispectral topographical features. The dominance of a few well defined ridges, troughs, peaks and hollows suggests line interactions among a few wavenumbers. The presence of a smoothly sloping or featureless terrain indicates continuum type interactions among most wavenumbers. At oceanic fronts, continuum type interactions predominate.

The normalized bispectra of temperature, salinity, sound velocity and density perturbations in the frontal region off northeastern Japan are shown in Figure 9 on the triple logarithmic scale. The dotted line denotes the Nyquist wavenumber line, beyond which the bispectrum is assumed to be vanishingly small. The computations were carried out in the wavenumber plane bounded by $|k_1| \leq 167$ c.p.km; $|k_2| \leq 167$ c.p.km; $|k_1 + k_2| \leq 167$ c.p.km, with an areal resolution of 48 (c.p.km)^2.

The outstanding feature is the rather smooth decay of the "third power density" from the origin to the Nyquist line. The total decrease covers three orders of magnitude. The rate of decrease is not uniform, however, but depends upon both wavenumber and direction, indicating anisotropic conditions. The decay coefficients for the "third power density" vary between -1 and -8 and tend to be largest, where the sum of the wavenumbers k_1 and k_2 lies between 60 and 100 c.p.km. In the high wavenumber region there are several rises and depressions superimposed on the smooth slopes. Because none of the topographical features depart

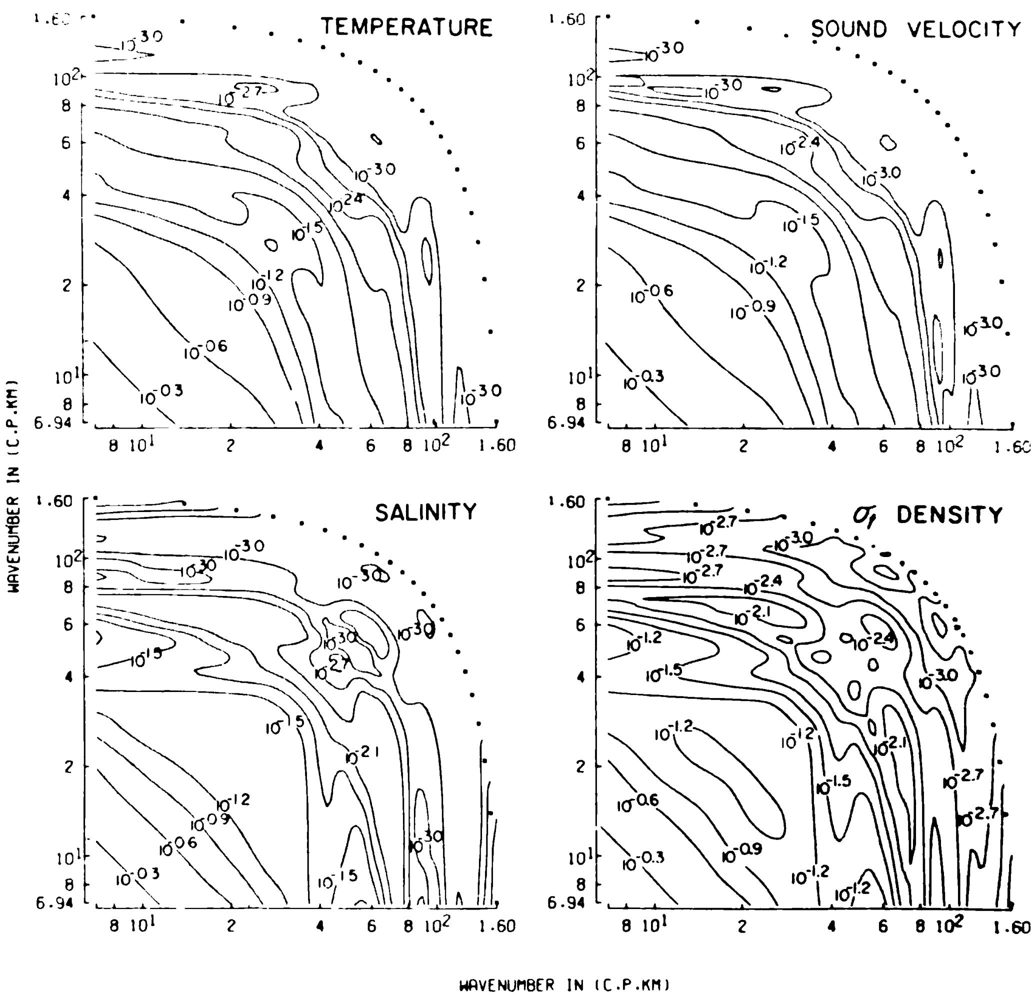

Figure 9 — Normalized bispectra of temperature, salinity, sound velocity and density corrected for binomial filtering. The dotted line refers to the Nyquist wavenumber.

much from surrounding terrain, they are statistically insignificant. The absence of significant ridges and depressions in the bispectra suggests that they result from continuum type interactions. The bispectra described could thus arise from turbulent interactions in an inhomogeneous medium, or from interactions of a *random* wave field in an inhomogeneous medium. The present data are insufficient to distinguish between these processes.

The Problem of Frontal Prediction

Fronts form, move, intensify, and decay in response to changing atmospheric and oceanic flow patterns. If the configuration of the velocity field, of the surface momentum, heat and salt flux fields were known with sufficient accuracy, fronts could be predicted in detail. For example, the intensification of the temperature front at a fixed geographical location could be predicted from

$$\frac{\partial}{\partial t}\left|\underline{\nabla} T\right| = -\frac{\partial v_n}{\partial n}\left|\underline{\nabla} T\right| - \frac{1}{\rho c_{vs}}\frac{\partial}{\partial n}\left(\frac{\partial q z}{\partial z}\right) - \frac{\partial}{\partial n}\left(\frac{\partial < w\,'T' >}{\partial z}\right)$$

where T is temperature, t is time, v_n is the velocity component normal to the front, positive in direction of increasing temperature, w is the vertical velocity, q_z is the vertical component of radiative heat flux, $< w\,'T' >$ is the vertical component of turbulent heat flux, all positive upware, ρ is density and c_{vs} is the specific heat of sea water at constant volume and salinity.

The terms on the right describe the various physical processes affecting frontal dynamics. These are, in sequence, velocity convergence in a region of existing temperature gradients, convergence of the radiative heat flux and convergence of the turbulent heat flux. The velocity convergence term is particularly large where currents of different origin meet. This happens not only at the confluence of the Kuroshio and the Oyashio, or of the Gulf Stream and the Labrador current, but also in mid-ocean, at convergence lines of wind induced Ekman transport. The radiative and turbulent heat flux terms are significant only in the upper oceanic layer. Their importance is larger at low than at high latitude fronts (7).

At present, meaningful prediction can be made only for fronts in the upper mixed layer in those parts of the ocean, where the baroclinic flow is weak. Then it is possible to use existing satellite and surface meterological information to delineate regions of frontogenesis and frontolysis. Because of the moderate dimensions of oceanic fronts (50-500 km) the meteorological information must be available on a space grid not coarser than a one-degree latitude-longitude grid.

For more accurate prediction of upper ocean fronts and for all cases of predicting fronts below pycnocline depth, it is necessary to know the configuration of the baroclinic flow field as well. This can be obtained only from a suitably dense network of *subsurface* temperature and salinity observations. Such information cannot be obtained from satellites, but requires use of ships and airplanes.

Conclusion

The study of ocean fronts is relevant for various purposes: (1) the thermohaline characteristics of the frontal zone are important for long range sound-transmission, (2) frontal zones are frequently regions of minimum hydrostatic stability, favorable for the development of turbulence and deep convection; (3) storms often form and travel along frontal zones, and (4) fronts are zones of particle convergence.

The presently available theories and observations have shown that oceanic fronts differ fundamentally from atmospheric fronts and require different methods of analysis. From a theoretical point of view, topographically bound fronts and the relation between multiple fronts and Rossby waves needs to be investigated more closely. From an observational point of view, the maximum horizontal gradients and their probabilities of encounter need be determined. From an operational viewpoint, frontal prediction requires timely information of the configuration of the surface energy flux fields (particularly the wind stress field), as well as satellite information on existing fronts.

References

1. M. Uda, 1938: "Researches on 'Siome' or Current Rip in the Seas and Oceans." *Geophys. Mag.*, **11**, 307-372.
2. E. Palmen and C. W. Newton, 1969: *Atmospheric Circulation Systems*. Academic Press, 602 pp.
3. G. I. Roden, 1972: "Temperature and Salinity Fronts at the Boundaries of the Subarctic-Subtropical Transition Zone in the Western Pacific. *J. Geophys. Res.*, **77**, 7175-7187.
4. H. E. Hulbert, 1974: "The Influence of Coastline Geometry and Bottom Topography on the Eastern Ocean Circulation." *Techn. Rep. Mesoscale Air-Sea Interaction Group*. Florida State University, Tallahassee.
5. H. Kawai, 1972: "Hydrography of the Kuroshio Extension." *Kuroshio*, H. Stommel and K. Yoshida, Ed. University of Washington Press, 235-269.
6. J. R. Luyten and A. R. Robinson, 1974: "Transient Gulf Stream Meandering; Analysis Via a Quasigeostrophic Time Dependent Model." *J. Phys. Oceanogr.* **4**, 256-269.
7. G. I. Roden, 1975: "On North Pacific Temperature, Salinity, Sound Velocity and Density Fronts and their Relation to the Wind and Energy Flux Fields." *J. Phys. Oceanogr.* **5**, in press.
8. G. I. Roden, 1974: "Thermohaline Structure, Fronts and Sea-Air Energy Exchange of the Trade Wind Region East of Hawaii." *J. Phys. Oceanogr.* **4**, 168-182.
9. M. Longuet-Higgins, 1965: "The Response of a Stratified Ocean to Stationary or Moving Wind Systems." *Deep Sea Res.*, **12**, 923-973.

10. J. Pedlosky, 1971: Geophysical fluid dynamics. *Mathematical Problems in the Geophysical Sciences, Lectures in Applied Mathematics,* 13, Amer. Math. Soc., 1-60.
11. H. G. Stumpf, 1975: "Satellite Detection of Upwelling in the Gulf of Tehuantepec, Mexico." *J. Geophys. Res.*, 5, 383-388.
12. H. G. Stumpf and P. K. Rao, 1975: "Evolution of Gulf Stream Eddies as Seen in Satellite Infrared Imagery." *J. Phys. Oceanogr.* 5, 388-393.
13. G. A. Maul and H. R. Gordon, 1975: "The Use of Earth Resources Technology Satellite (LANDSAT-1) in Optical Oceanography." *Remote Sensing Environment*, 4, 95-128.
14. D. B. Miller, 1971: *Global Atlas of Relative Cloud Cover 1967-70, Based on Data on Meteorological Satellites.* National Environmental Satellite Service, Washington, D.C. 273 pp.
15. G. I. Roden, 1971: "Spectra of North Pacific Temperature and Salinity Perturbations in the Depth Domain." *J. Phys. Oceanogr.*, 1, 25-33.
16. G. I. Roden and D. J. Bendiner, 1973: "Bispectra and Cross-Bispectra of Temperature, Salinity, Sound Velocity and Density Fluctuations with Depth Off Northeastern Japan." *J. Phys. Oceanogr.*, 3, 308-317.
17. M. C. Gregg, 1975: "Oceanic Fine and Microstructure." *U.S. National Report, 1971-1974. American Geophysical Union*, Washington, D.C., 586-590.
18. J. W. Tukey, 1965: "Data Analysis and Frontiers of Geophysics." *Science*, 148. 1283-1289.

Cause of the Loop Current in the Gulf of Mexico

Wilton Sturges of Florida State University has observed that the flow into the Gulf of Mexico, through the Yucatan Channel, appears to have a typical seasonal maximum in May or June, on the basis of the climatological mean temperature distribution between Cuba and the Yucatan Peninsula. The flow into the Straits of Florida, however, appears to have its seasonal maximum between June and August, depending on the data base used. The formation of the Loop Current in the Gulf of Mexico appears to result from the accumulation of Loop Current water, caused by the phase shift of approximately a month between inflow and outflow.

The sea-level slope between the Gulf and open Atlantic will be a function, among other factors, of the height of sea level along the west coast of Florida. Such coastal sea levels are known to be dominated (for periods of a month or less) by longshore winds on a scale of a few hundred km. The extent to which the Loop Current itself affects sea level is not known. The mass transport flowing into the Gulf will be determined by some integrated measure of the Trade Winds. The Trades will be coupled only very loosely to the winds on the west coast of Florida. It seems reasonable to expect, therefore, that there may be large variations in the Loop Current from one year to the next.

Large Scale Variations of the Temperature Field in the North Pacific Ocean

T. P. Barnett*
Scripps Institute of Oceanography

Introduction

After decades of exploration, oceanographers have obtained a fair idea of the average properties of the North Pacific Ocean. This knowledge has been gained almost exclusively through numerous cruises of observation. However, only in the last few years has the data been sufficient to begin to focus on the *variability* associated with the mean fields. Recent studies indicate a degree of large scale variability that was not expected. It is thus clear that the study and eventual explanation of fluctuations in ocean properties will be one of the most exciting and rewarding aspects of physical oceanography in the years to come.

An important class of field variation is the large scale, interannual fluctuations in the near surface thermal field of the central North Pacific Ocean. These fluctuations typically have a magnitude up to 3°C which is approximately 30 - 40% of the seasonal signal. They occur over space scales of the order of 1000 or more kilometers. The changes are accompanied by equally large changes in the climate of both the ocean and the atmosphere, in the geographical displacement of biological species, a redistribution of mass in the upper levels of the ocean and presumably a baroclinic adjustment of the ocean circulation to this shift in mass. These general remarks are based on observations of sea surface temperatures and fragmentary histories of the sub-surface temperature structure. A good history of the variation of temperature at depth is not currently available.

A program has been established within the North Pacific Experiment (NORPAX) to remedy the lack of observational evidence on subsurface thermal variability. The observational aspect of the program uses Navy Fleet P-3's to routinely survey the temperature regime in the central ocean. The aircraft have, for the last year, occupied standard meridional sections between Adak and Honolulu deploying airborne expendable bathythermographs (AXBT's) at fixed locations along each section.

*Dr. T. P. Barnett is well-known for his studies of ocean wave structure. Recently he has concentrated on managing the NORPAX project and applying modern statistical techniques to upper ocean data. He is a senior research associate at Scripps Institute of Oceanography.

These north/south sections, which run in the direction of the maximum sea surface temperature gradient, thus provide information on the monthly, seasonal and interannual variability of the central ocean's temperature field. These data are contributing to a picture of the ocean's thermal field that has not previously been observed.

This paper will present a brief discussion of the experimental method and instrumentation used in the aircraft program. Finally the paper will describe some of the results to data by presenting information on frontal motion, vertical profiles of temperature structure beneath sea surface temperature (SST) anomalies and a *partial* discussion and evaluation of the mechanisms that might explain the observed changes in heat content.

Instrumentation

The principal device used in this study is a Navy Fleet P-3C (Figure 1). These aircraft have a range exceeding 3,000 miles and are thus an ideal tool for quickly mapping the vast regions of the central Pacific. The planes have the capability to launch AXBT's and record the resulting data on temperature as a function of depth on magnetic tape. Their navigation systems include both inertial, Doppler, Loran, and other standard devices such that positional accuracy of ± 2 miles is realizable. This has allowed us to go back to virtually the same spot in the ocean,

Figure 1 — A Fleet P-3.

month after month, to repeat our observations. This unique opportunity makes it possible to look at the natural variability of the temperature field without having to worry about apparent variability induced by non-uniform spatial sampling.

The second component of our instrumentation is the airborne expendable bathythermograph. This device is launched from the aircraft and upon striking the water, releases an end plate on the bottom of the AXBT. The following sequence of events then usually occurs: A salt water battery is flooded, providing power for the system; an antenna is deployed from the top of the floating AXBT; a sensing probe is released from the main housing, measuring temperature as it falls; this information is transmitted back up a wire connecting the falling probe with the remaining surface float; the information is used to modulate a radio transmitter whose signals are in turn received by the aircraft. The frequency of the radio signal is proportional to the temperature of the water.

Considerable effort has been put into determining the constant of proportionality mentioned above. With earlier AXBT's it was necessary to calibrate each instrument since no reproducable calibration coefficient could be found that met the required accuracy standard (± 0.2°C). Newer units, however, are uniform in their character so that it is possible to define a universal calibration for all of the systems. This new calibration curve, while not identical to that provided by the manufacturer, can be applied to all units and provide the accuracy required (see Figure 2). A full description of the calibration procedure and results may be found in Sessions, *et al* (in press).

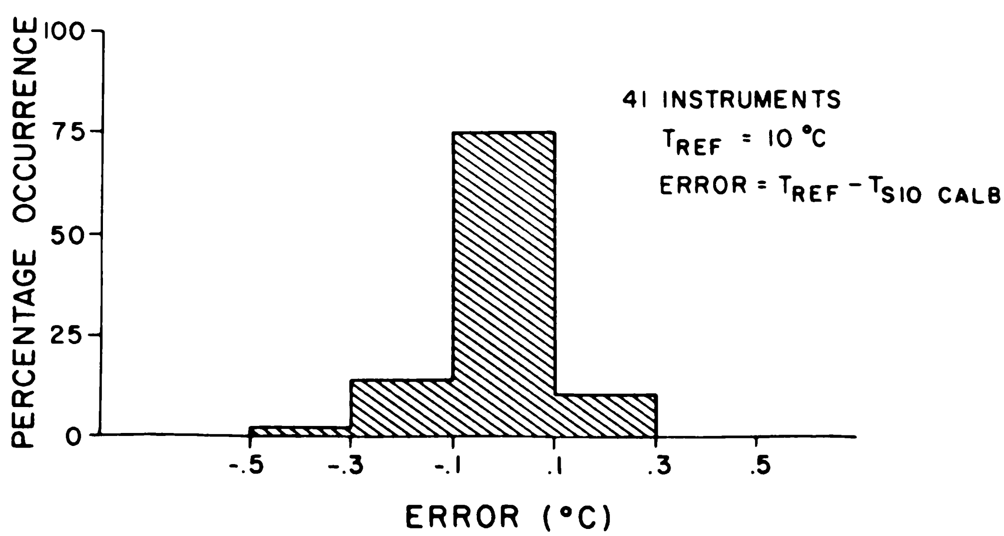

Figure 2 — Differences (errors) between SIO calibration curve ($T_{SIO\ CALB}$) for Magnavox AXBT's and actual values (T_{REF}).

The Fleet aircraft provide the opportunity to cover vast stretches of the ocean, returning with excellent accuracy to the same location time after time to repeat a set of observations. The measurement tool itself, the AXBT, can be calibrated to provide accuracy that is adequate for our present investigations. The errors in measurement are a factor of 10 less than the signal to be observed.

Methods

Our experimental procedure is simple. Each month a Fleet P-3 leaves Adak in the Aleutian Chain for the position 50°N, 158°W. Upon reaching this location the plane turns south along the 158th meridian, dropping an AXBT every 80 kilometers until measurements are terminated at latitude 30°N.* The plane continues on to the Hawaiian Islands. After a day's layover in Honolulu the plane returns to Adak via Midway, this time along longitude 170°W. AXBT's are again dropped every 80 kilometers between latitudes 30° and 50°N. A typical flight track and examples of the data obtained during a flight are shown in Figure 3.

An on-board Scripps engineer insures data quality by comparing the measurements, as they are taken, with long term means. He also insures the data is properly recorded on a digital data logging system developed at Scripps Institution of Oceanography. Upon completion of each flight, the digital data tapes (cassettes) are played through a Super NOVA computer for preliminary data editing, addition of identification information, and conversion to 9-track tape. The data is then subject to visual and numerical inspection via an interactive CRT display system. Any editing that may be required, and it is generally very small, is made through the interactive terminal. The data are then transferred to permanent storage on a Control Data 7600 and available for processing. The two editing sequences, tape conversion, and transfer to the CDC-7600, take approximately one man-day.

The survey operation has been reduced to a routine level. Sophisticated data recording and editing schemes have been developed so that only a small effort is required to deal with the large volume of data generated by each flight.

Initial Results

The observational program is in full stride and much data remains to be collected. Nevertheless, some rather startling, though preliminary, conclusions can be drawn from the data collected so far. In this section

*The sampling scheme was derived from consideration of (1) availability of historical data, (2) spatial temperature variance analysis, (3) scale studies of the POLE program and (4) optimal sampling theory.

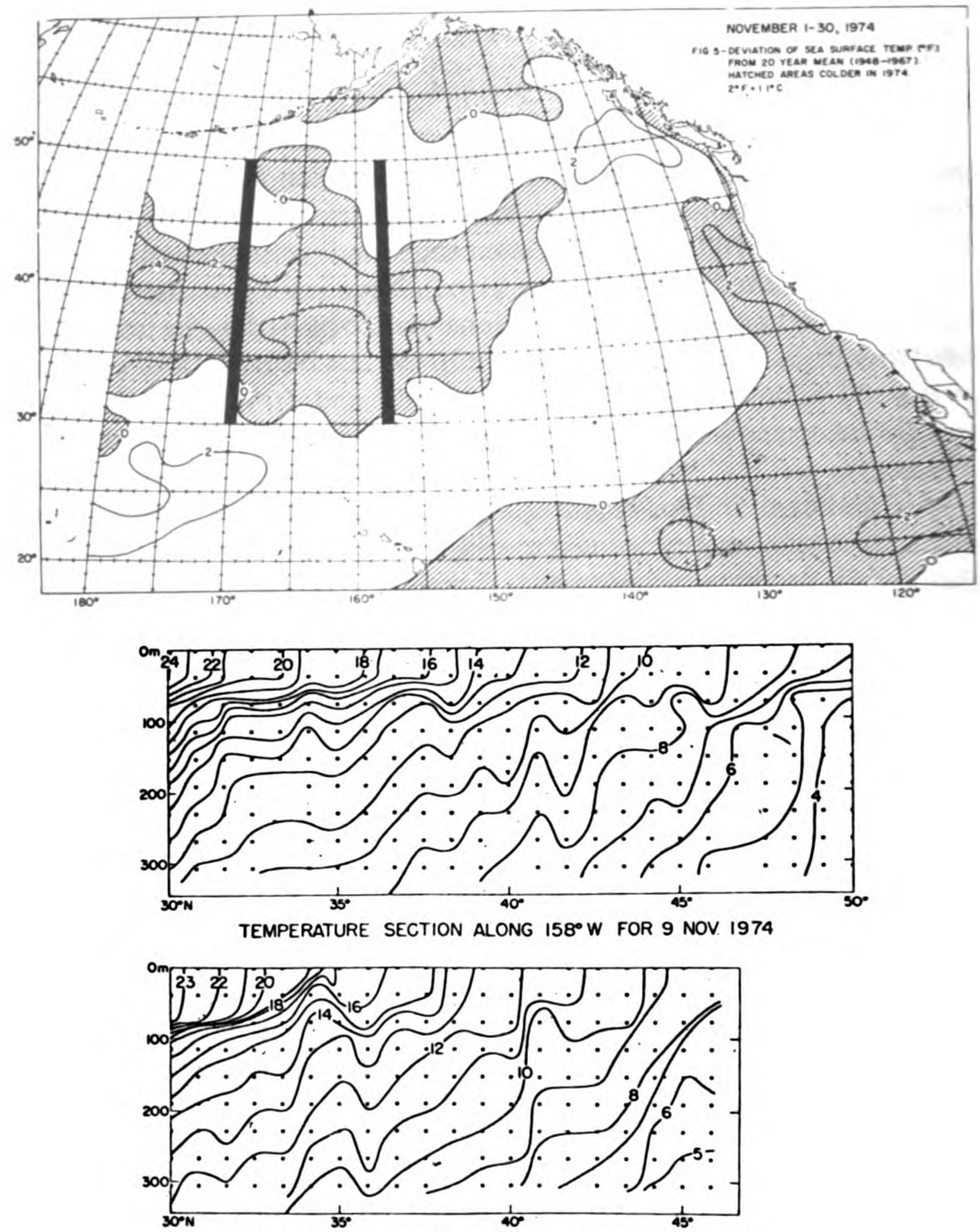

Figure 3 — Upper: Flight track superimposed on monthly map of SST anomaly. The map comes from the National Marine Fisheries Service (NMFS). The shaded areas are colder than the long term average for the month. Lower: Typical temperature fields obtained along a standard section.

we will (1) view some examples of large scale temperature variability, (2) obtain a first picture of the vertical extent of SST anomalies, and (3) examine some of the physical processes that might account for the observed changes in heat content. Space limitations require these discussions to be brief.

Examples of Large Scale Variability

Two typical examples of the large scale space/time variability are being documented. The examples are intended to give the reader a feeling for the magnitude of the phenomena being studied and hence an appreciation for their importance.

The first case study (Figure 4a) shows the result of simply subtracting the 170°W section data obtained in February 1975 from the same section data obtained in November 1974. Note the seasonal cooling ($T_{Nov} > T_{Feb}$) is confined to the near surface area above 100 m, about as expected. The largest change in near-surface heat content occurs near 30°N instead of further north as might have been anticipated. More interesting is the relatively large increase in temperature ($T_{Nov} < T_{Feb}$) at depth. The warming occurs all the way to 300 m, the limit of measurement. The amount of apparent warming is a factor of 10 greater than called for in many oceanographic text books. Perhaps most surprising is the fact that the *total* heat content in the section is slightly *greater in February* than in November, a situation which seems to contradict present oceanographic dogma.

The second example demonstrates not only the variability of the ocean but also the great utility of aircraft as a measurement tool. Figure 4b shows the position of the Subtropical Front at each meridian as a function of time. The Front was defined simply by a maximum in the North-South temperature field gradient at 100 m depth. The movements of the Front are up to 300 km from what appears to be a preferred position near 32°N. The time scale of the motion suggest a regular seasonal march although the time series is not long enough to substantiate this notion. Work is in progress to relate the variations in Frontal Position to the local wind field. The first task, however, is to properly define the Frontal region, for the idea of representing it as a single discontinuity in the temperature field is highly idealized. The ocean is, unfortunately, more complicated.

Beneath an SST Anomaly

It has been possible to obtain an initial picture of the subsurface character of SST anomalies. This description has suggested possible causes for the anomalies but at the same time has raised more questions about them than it has answered.

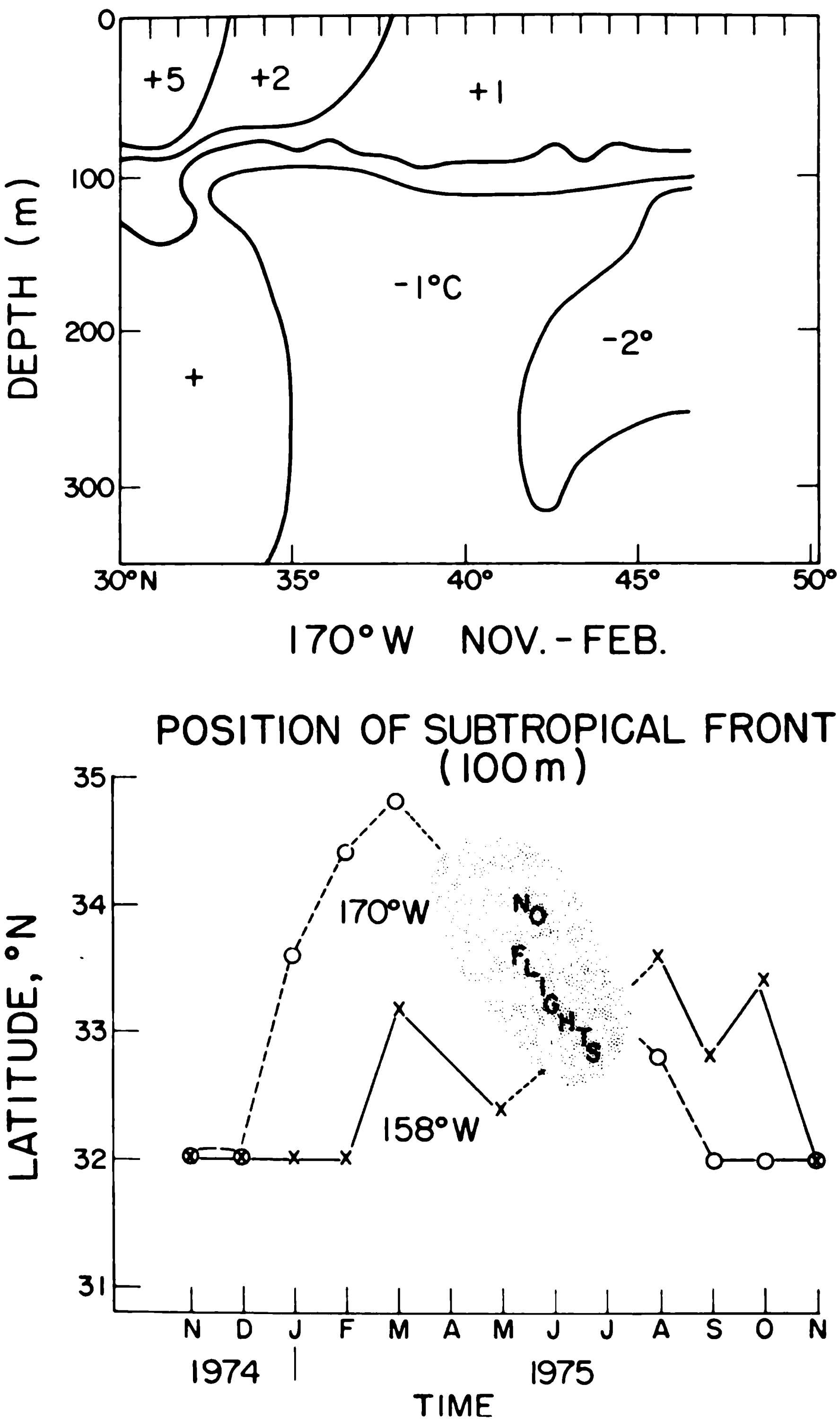

Figure 4 — (a): The change in temperature between November 1974 and February 1975 along 170°W. A '+' indicates November was warmer than February. (b): The latitudinal position of the Subtropical Front between November 1974 to November 1975 at longitudes 150°W and 170°W.

The results shown below owe much to (1) the timely occurrence of large anomalies in the vicinity of our flight tracks (Figure 3) and (2) to the generosity of R. Bernstein and W. White who made available their preliminary estimate of the long term average or mean properties of the subsurface temperature field in the central Pacific. Subtracting the mean field from the observation gives the 'anomaly' field discussed below.

Selected meridional sections through SST anomalies have been spatially smoothed and are shown in Figure 5. These sections were chosen to show different types of situations that have been observed, i.e., they are 'typical.' In viewing this illustration it will be helpful to know that typical standard deviations associated with the long term mean fields are roughly 1°C at the surface, 1°C at 100 m and 0.7°C at 250 m. The major features of the illustrations are clearly significant and suggest the following hypotheses:

Upper Panel: The major anomaly is confined to within 60 m of the surface and, in a sense, resembles the 'cold pool' concept presented earlier in numerous publications by Namias (e.g., 1970). This close association suggests the anomaly is caused by an unusually large air/sea heat exchange, i.e., it is atmospherically induced. More will be said on this matter subsequently.

Middle Panel: One month later the anomaly has decreased at surface but increased in intensity at depth, particularly between latitudes 35° and 40°N. This geographic region is noted for its low hydrostatic stability (Roden, 1970) which suggests that penetrative convection may have been a prime mechanism in causing the intensification at depth.

Lower Panel: This field is typical of the period August-October 1975 along both meridional sections. The persistence of the field over 3 months amply demonstrates the oft-mentioned 'oceanic' memory. At the same time it illustrates the fact that the ocean can disguise its true summer character beneath a thin surface layer. In this particular case, the small negative anomaly at the southern end of the section hides a thick layer of water that is up to 2-3°C warmer than the long term mean. Apparently this additional heat is due to a deeper than usual mixed layer, a situation which existed over most of the central Pacific during August-October, 1975.

SST anomalies seem to be accompanied by at least several classes of subsurface temperature field. This suggests more than one physical mechanism may be principally responsible for their creation. Nevertheless, explanations for the subsurface anomalies must be found for they often extend through the mixed layer to at least 300 m depth. They thus represent a considerable perturbation in the ocean's near-surface sound velocity field and perhaps the density field also.

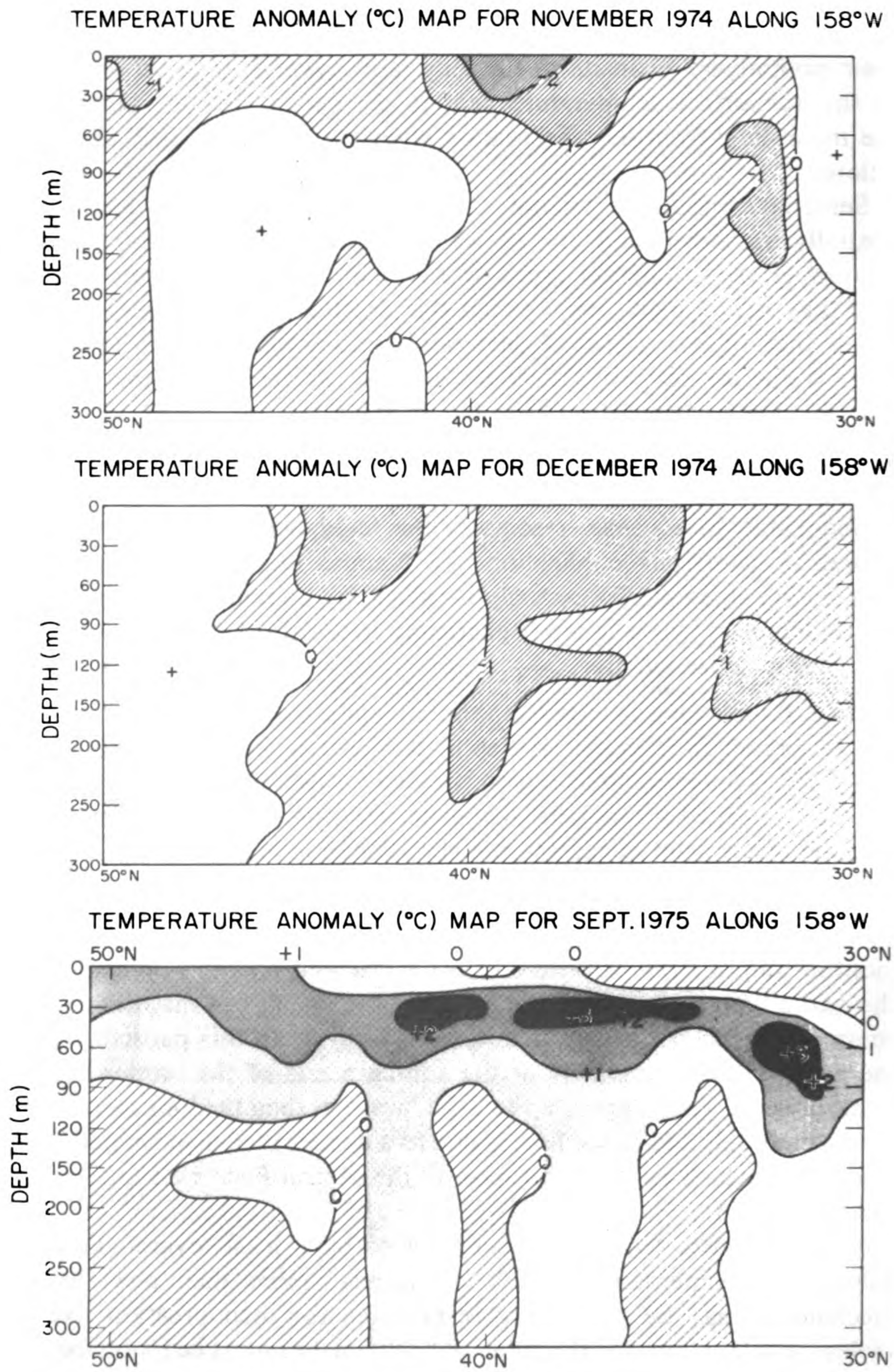

Figure 5 — Three classes of subsurface temperature anomaly. Each suggests different mechanisms of generation.

Examination of Processes

Numerous physical mechanisms could cause the observed changes in near surface thermal field. Although the processes probably act in combination, as suggested above, we are examining them individually with the hope of finding a dominate mechanism. A preliminary analysis has been completed for the processes of air/sea heat exchange and Ekman pumping and these are discussed below. Other processes, e.g., horizontal advection, mixing, etc., are currently under study and will be discussed elsewhere.

The discussion is conveniently framed in terms of the heat conservation equation

$$\frac{\partial H}{\partial t} + \nabla \cdot (VH) + \nabla \cdot (\nabla AH) = \Sigma_i \, Q_i \qquad (1)$$

where it is understood that all variables depend on space and time. The physical meaning of the terms is

(1) $\frac{\partial H}{\partial t}$ = local rate of change of heat content, H.

(2) $\nabla \cdot (\underset{\sim}{V}H)$ = advective flux of heat, both horizontal and vertical, by ocean currents, $\underset{\sim}{V}$.

(3) $\nabla \cdot (\nabla AH)$ = horizontal and vertical flux of heat by mixing processes. A is the 'mixing' coefficient.

(4) $\sum_i Q_i$ = summation of air/sea heat exchange processes at the ocean's surface.

Air/Sea Heat Exchange

A simple explanation for the changes in oceanic heat content involves the transfer of heat from (to) the ocean to (from) the atmosphere. Other processes within the near surface layers of the ocean act in consort, to establish a well mixed layer from which this heat is extracted (added). The resulting balance equation, with standard approximations, for a layer of water in contact with the atmosphere reads

$$\frac{\partial H}{\partial t} = \pm \sum_i Q_i$$

The key question is: Can the total heat lost (gained) by the near surface layer of the ocean in the interval between data gathering flights be equated to the heat gained (lost) by the atmosphere during the interval?

An answer to the above question requires an evaluation of the ΣQ_i. This was done in two ways using *only present operational* sources: (1) The 'bulk' formulae for air/sea heat exchange are routinely evaluated by the National Marine Fisheries Service, NMFS, (Clark, *et al*, 1974).

This estimation involves the use of monthly values of such descriptors as SST, air temperature, wind speed, etc., in simple formulae to obtain ΣQ_i. This approach is regularly critized on grounds that (a) calculations using the monthly means of SST, etc., do not adequately represent the (intermittent) flux processes and (b) the bulk formulae are grossly inaccurate. Recent work of Friehe and Schmitt (in press) shows the latter criticism to be less important than previously thought. Calculations (not reported here) show that (a) induces errors of order 30% in the estimate of ΣQ_i. (2) Air/sea heat exchange are routinely computed by an atmospheric global circulation model operated by the Fleet Numerical Weather Central, FNWC (Kesel and Winninghoff, 1972). The model has the advantage that it incorporates actual observations of air temperature, etc., into its computed fields. The resulting estimates of the fields important to ΣQ_i are thus based on real data that has been smoothed and interpolated with the Navier-Stokes equations. The equations used in the model to estimate ΣQ_i were originally due to Arakawa and not easily judged in this article. The FNWC estimates of ΣQ_i are available every 12 hours, an interval which should satisfy the objection (a) above.

The operational estimates of ΣQ_i are compared in Figure 6 with actual measurements of heat loss (gain) in the ocean's upper 100 m for the Fall/ Winter of 1974-75. The illustrations clearly demonstrate that neither operational estimate of air/sea heat exchange comes consistently close

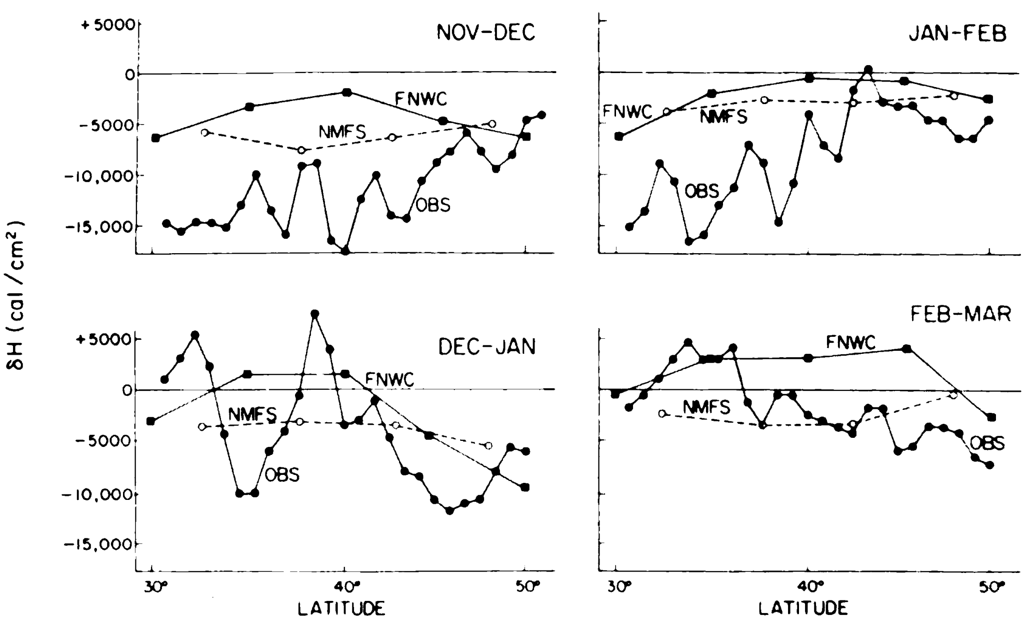

Figure 6 — Estimates of air/sea heat exchange from the operational products of Fleet Numerical Weather Central (FNWC) and NMFS compared with observed heat losses for the winter 1974-75. The products do not generally account for the observed loss.

to explaining the observed heat changes. Also, the spatial character of actual heat loss, and even the direction of the flux, are not particularly well represented.

Let us suppose that air/sea heat exchange is, in fact, a dominant mechanism in creating SST anomalies and associated changes in the near-surface temperature field. The above results show that, with operational tools, we can only estimate the exchanges to within a factor of 3. This is not good enough to explain quantitatively the anomalies, let alone predict them. If, on the other hand, we suppose that the estimates of air/sea heat exchange are accurate to, say, $\pm$ 50%, then other physical processes must be playing a dominant role in controlling the oceanic heat budget. In any case, a special set of observations and/or highly refined analysis techniques will be required to determine how good the estimates of large scale air/sea heat really are. Work in the area does not appear to be progressing rapidly.

Open Ocean Upwelling

An 'in-vogue' mechanism used to explain large changes in heat content is upwelling/downwelling or simply 'Ekman pumping.' In the open ocean, large storms are thought to set up a near surface circulation that gives rise to either upwelling or downwelling. This comes about since the Ekman transport, being directed perpendicularly to the right of the wind stress vector, will carry water away from (toward) the center of a cyclone (anticyclone). The resulting divergence (convergence) gives rise to a vertical motion of water, w, which works against the vertical temperature gradient to transport heat. A vertical displacement of isotherms is generally used to infer the sense of the vertical motion since w is very difficult to measure.

The balance equation representing this process is

$$\frac{\partial H}{\partial t} \doteq - w \frac{\partial H}{\partial z}$$

where w is positive upwards. Knowing the wind field, it is possible to estimate w by invoking the well known, theoretical relation

$$\frac{\text{curl } \tau}{\rho f} = w$$

where τ is the vector wind stress and f the coriolis parameter. The above neglects any contributions from the divergence of geostrophic flow.

Using 12 hourly estimates of $\underset{\sim}{W}$ from FNWC, we have selected for study a period during the winter 1974-75 of unusually steady atmospheric circumstances over the North Pacific Ocean. The nature of the wind field is shown in Figure 7. The u-component has the classical 'half wave'

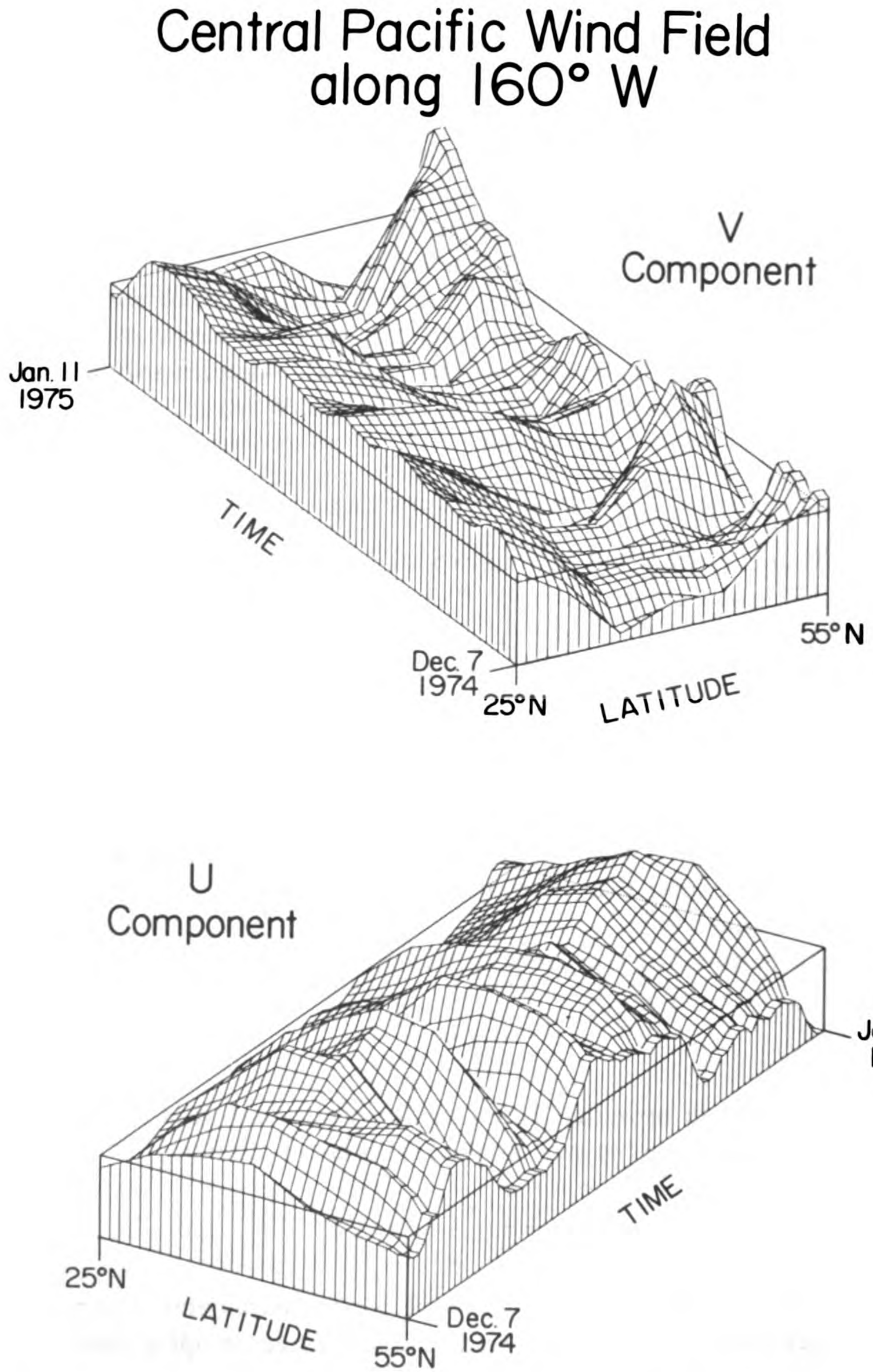

Figure 7 — Latitude/time projections of the U and V components of the FNWC-estimated wind along 160°W during Dec-Jan 1975. The wind field is quite uniform in time and rather simple in spatial character.

shape with a maximum (ridge) near 40°N. The v-component is virtually the same but in anti-phase. Both of the patterns are remarkably constant in time and, as additional data showed, quite uniform in the east/west direction. Such a stable, but simple, circulation pattern offers an excellent opportunity to test the Ekman pumping idea.

The average value of w over the measurement interval was computed from the above relation. It is shown vs latitude in Figure 8. Remember that positive values of w represent upward vertical motion and hence cooling. Also shown are the observed heat changes during the period in the layers between depths 0-100 m and 200-300 m.* It will be helpful for comparison purposes to know that $w = 5 \times 10^{-4}$cm/sec is equivalent to a value of δH in the 200-300 m slab of approximately -2000 cal/cm².

The values of w are generally low, but order of magnitude-adequate, to explain the heat changes. Unfortunately, the spatial distribution and sign of w are not similar to that of heat loss. These same remarks hold for the other months that were investigated. Combining air/sea heat exchange and Ekman pumping will help explain some of the observed heat losses. There remain, however, numerous cases where order of magnitude agreement cannot be found. In any event the comments about the mismatch in space scales between observed and computed heat loss are unaltered.

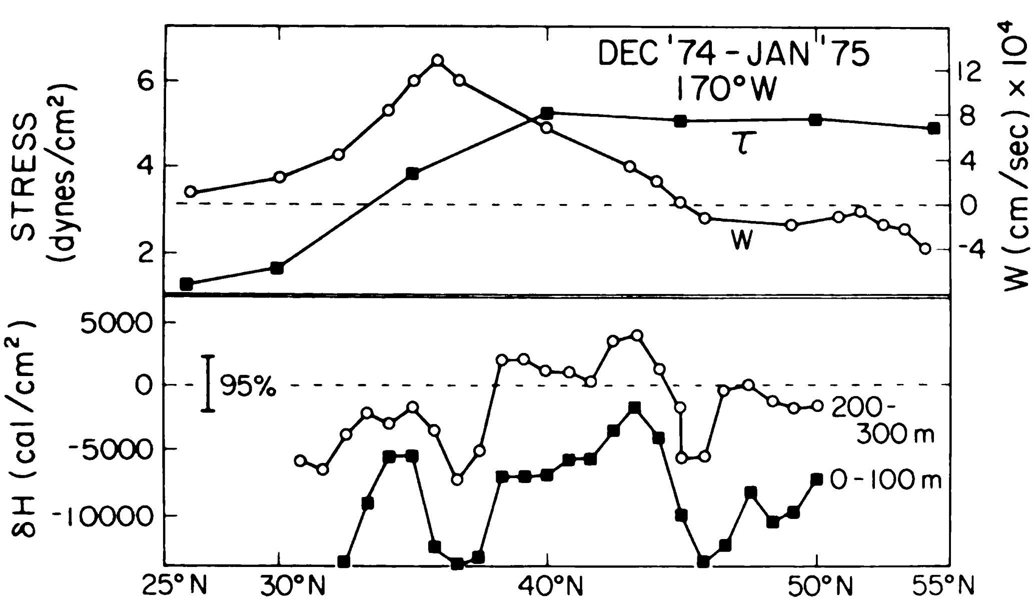

Figure 8 — Comparison of monthly mean estimates of vertical motion (w) and wind stress (τ) with observed oceanic heat changes. The process of upwelling/downwelling, as inferred from the distribution of w, appears to be of questionable importance to the oceanic heat budget.

*The layer between 100-200 m behaves like the 200-300 m layer.

This very simple case, and other more complex situations that we have investigated, *tentatively* suggests the Ekman pumping mechanism is not one of the more robust terms in the heat budget equation. To verify this conclusion it will be necessary to actually measure the near surface currents over long periods of time in conjunction with observations of the temperature field. Two programs within NORPAX are now obtaining the required current measurements. If they are successful, we can look to these combined measurement programs for some highly significant results.

Summary

Large scale fluctuations in the thermal field of the central Pacific Ocean are being routinely measured with AXBTs deployed by Fleet P-3s. The observations indicated the presence of big interannual signals in the temperature field. These variations, which are coherent over large distances, can be as large as 30-40% of the seasonal signal. They thus represent a significant perturbation to the temperature field in the near-surface region.

The measurements suggest several physical mechanisms that may be generating the month-to-month variations in the near-surface temperature field. Two particular physical processes suggested by the data have been examined in relation to observed changes in the oceanic heat content. (1) Air/sea heat exchange offers an order of magnitude explanation for some, but not all, of the changes in heat content in the ocean's upper 100 m. Better atmospheric data and analysis techniques will be required to improve quantitatively the explanation. (2) Ekman pumping (upwelling/downwelling) offers an unsatisfying explanation for most of the observed change in the deeper thermal structure. However, direct observations of the near-surface current are required to probe further into the importance of this process. In summary, a convincing explanation of the observed change in oceanic heat content was not found via these two mechanisms. Work is in progress to evaluate the other physical processes embodied in equation (1).

Measurements of the type described in this article are opening the way for physical oceanographers to study macroscale ocean/atmosphere processes. Such studies will be immensely rewarding over the next decade. One of their major payoffs will be in providing a perspective for where physical oceanographers should be concentrating their efforts. With proper support and guidance, the next generation of physical oceanographers may, in fact, feel comfortable in discussing and investigating the macrophysics of an entire ocean basin. We would then be only some 40 years behind meteorologists in our approach to and concept of how ocean physics might be studied.

References

N. Clark, L. Eber, R. M. Laurs, J. A. Renner and J. F. T. Saur, 1974. "Heat Exchange Between Ocean and Atmosphere in the Eastern North Pacific 1961-71." *NOAA Tech. Report* NMFS SSRF-682, pp 108.

C. A. Firehe and U. Schmitt, 1975. *Parameterization of Air-sea Interface Fluxes of Sensible Heat and Moisture by Bulk Aerodynamic Formula.*

P. Kesel and F. Winningkoff, 1972. *Monthly Weather Review*, **100**(5): 360-73.

J. Namias, 1970. *J. Geophys. Res.*,**75**(3): 565-581.

G. Roden, 1970. *J. Geophys. Res.*, **75**(6): 1097-1109.

M. H. Sessions, T. P. Barnett and W. S. Wilson, 1975. *The Airborne Expendable Bathythermograph. Deep-Sea Research* (in press).

Ocean Leveling

For the last 50 years, the results of geodetic leveling on land have shown an apparent rise of sea level from south to north. The most recent work (1973) found a full meter of sea-level change between San Diego and the Canadian border. One of our ONR contractors, W. Sturges, has challenged the leveling result since 1966, in a number of papers (Ph.D. dissertation, 1966; J. Geophys. Res., 1967; Deep-Sea Res., 1968; J. Geophys. Res., 1974; Deep-Sea Res., 1974; and a number of presentations). The basis of the challenge was that the slope suggested by the land leveling could not be reconciled with our understanding of the dynamics of ocean circulation. He put forward the suggestion that perhaps an undetected systematic error was present in the leveling work. This suggestion was not received warmly by the levelers.

In February 1974, Sturges invited several physical oceanographers and geodesists to a small workshop, under ONR sponsorship, at the Rockville, Maryland headquarters of the National Ocean Survey (formerly the U.S. Coast and Geodetic Survey). Specific experiments and analysis schemes were proposed at that workshop through which the levelers could examine their existing lines for a systematic error. These analyses have recently been completed. At a special meeting of the AGU Committee on Marine Geodesy, held last year, Mr. Emory Balaxs, of the National Ocean Survey presented the results of his work, which clearly show the presence of a systematic error—of precisely the correct magnitude and sign to account for the discrepancy between the land leveling and the oceanographic calculations.

Removal of the systematic error will now allow the results of land leveling to be used to connect coastal tide gauges, to furnish direct observations of the absolute pressure gradient at the sea surface. These results will not only be applied to several problems in ocean circulation but to the new high precision satellite altimeters such as the one now being flown in GEOS 3, which will require "ground truth" calibration in attempts to determine the geoid to an accuracy of approximately 20 cm. With the resolution of this coastal leveling problem, a major obstacle in the interpretation of satellite geoid data has been removed.

Physical Oceanography in the AIDJEX Program

Kenneth Hunkins*
Lamont-Doherty Geological Observatory

Sea ice varies greatly in seasonal extent, covering the entire Arctic Ocean during winter months, but shrinking during summer to cover only 60% of the ocean. On the geological time scale even larger changes in area take place. It has been shown that polar waters (less than 0.5°C) invaded the North Atlantic during the Wisconsin ice advance. This implies a much greater ice cover on the oceans during that period than now (Ruddiman and McIntyre, 1973). Moreover, sea ice has a large potential for changing climate through its high albedo, reflecting up to about 75% of incoming radiation, in contrast to only 10%-20% for open water. Thus radiation exchange in the polar regions is altered drastically by the presence or absence of pack ice. This change in ice extent and its importance to the radiation balance suggest that it has a role in feedback processes leading to climatic change.

There are strong differences of opinion on the role of the Arctic Ocean in global climate changes. According to some theories the ice-ocean-atmosphere system is inherently bistable and capable of switching from ice-covered to ice-free conditions with only a small triggering influence. Such a switch would undoubtedly produce profound changes in the climate of the northern hemisphere. Others have maintained that the present ice pack is stable, so that even if it were removed by some means, natural or artificial, it would reform and return to its original state. The uncertainties in our knowledge of fluid dynamics on a global scale do not yet allow a choice between these divergent theories.

Little is known about the behavior of sea ice on a large scale. The opening of leads and production of pressure ridges introduce complications. In order to improve our understanding of arctic pack ice and of the oceanic and atmospheric processes associated with it the Arctic Ice Dynamics Joint Experiment (AIDJEX) was conceived in 1970. The concept of AIDJEX grew out of the realization that isolated drifting research stations, which have been maintained by both the United States and the Soviet Union in the Arctic Ocean over the past quarter of a century, were inadequate for answering questions about the large-scale deformation of sea ice. A multiple-station array is required to

*Dr. Kenneth Hunkins is a physical oceanographer at Lamont-Doherty Geophysical Observatory, Columbia University. Dr. Hunkins, who is a renown arctic oceanographer, has discovered messoscale eddies in the Arctic Ocean.

measure the strain of the ice pack under the stresses exerted on it by winds and ocean currents. Such an array of manned scientific stations and automatic data buoys was deployed in March, 1975 and will continue in operation until April, 1976. These field experiments are combined with development of a numerical computer model of ice deformation. The results should ultimately lead to a predictive sea ice model that can be coupled with numerical global atmospheric and oceanic models to represent the behavior of the fluid earth (Maykut et al., 1972).

AIDJEX is a cooperative effort of research groups from universities, government agencies and industry, coordinated by a central staff with headquarters at the University of Washington. An information bulletin is published at intervals, and a data bank is maintained at the AIDJEX office in Seattle. The primary numerical modeling effort is also located there. Funding comes primarily from the Office of Naval Research and the National Science Foundation with additional smaller amounts from other government agencies. In addition to the United States, Canada has participated heavily in both preliminary scientific studies and logistic operations. Japanese scientists have taken part in a pilot program, and the Soviet Union has sent visitors to a pilot station.

The Arctic Ice Dynamics Joint Experiment will be integrated with two other large-scale experiments to monitor the dynamics of global circulation. These are the forthcoming Global Atmospheric Research Program (GARP) with tropical "experiments" in the earth's heat source region and the Polar Experiment (POLEX) put forward by the USSR as a comprehensive program for monitoring ocean-atmosphere interaction over the polar heat sinks.

Three AIDJEX pilot studies have been conducted in the Arctic Ocean, each for a period of one or two months, in 1970, 1971 and 1972. The 1972 pilot program involved over 80 persons in the largest and most complex scientific project on drifting ice ever undertaken by the United States. Three manned stations were situated in a triangle 100 kilometers on a side, positioned by satellite navigation and acoustic bottom transponders. The stations moved generally westward with the average ice drift in this region, covering about 100 kilometers in seven weeks.

The main AIDJEX field program began in April, 1975 and will continue for one year. Four manned ice stations were established in an array with a spacing of 100 km. One of the ice camps is viewed from the air in Figure 1. The original locations of the stations and their positions after drifting for seven months are shown in Figure 2. Each station is equipped with a satellite navigation system providing positions with an estimated accuracy of ± 10 m. A program of surface weather observations is also carried out at each station. At the main camp there are additional programs for measuring wind stress on the ice. Surrounding

Figure 1 — View from the air of the main AIDJEX ice station, Big Bear, during summer, 1975.

the array of manned ice stations is a circle of automatic data buoys recording position, barometric pressure and temperature dates. Two types of buoys are employed, one with a high frequency radio link telemetering data to the main camp and the other telemetering data back to a land station via a satellite link.

The AIDJEX oceanographic program has the objective of measuring water stress on the underside of pack ice and of providing information on how water drag behaves under various conditions of ice speed relative to the water, ice roughness and the stability of the water column. This requires observations of the basic oceanographic parameters of velocity, temperature and salinity in the upper layers. A program of daily profiles of currents, temperature and salinity is carried out at each of the four camps. Continuous profiles of ocean current are obtained with Savonius rotor meters which are lowered to 200 m and raised again at the slow rate of 5 m/min. In addition two Savonius rotor current meters fixed on inverted masts record currents continuously at depths of 2 and 30 m. below the base of the ice. Salinity and temperature are monitored by daily casts to 1000 m with Plessey 9040 Salinity-Temperature-Depth recorders (STDs). The STD casts are calibrated with reversing thermometer readings and salinity values from bottle samples run on a laboratory salinometer.

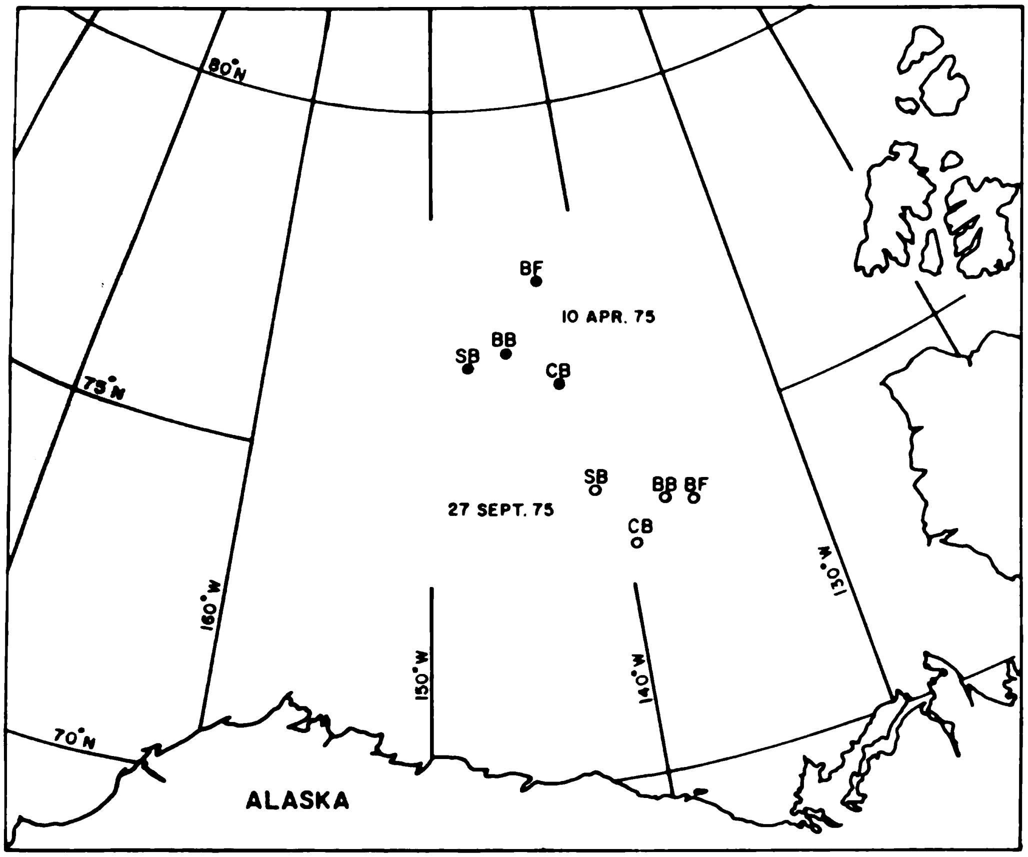

Figure 2 — Original sites of the manned AIDJEX stations and their locations after seven months of drift. The station names and abbreviations are: Big Bear (BB), Snowbird (SB), Caribou (CB), and Blue Fox (BF).

Water stress is generally a drag force on the ice. Momentum flows downward from the wind to the ice and then to the ocean. Momentum flux is downward through the base of the ice into the oceanic boundary layer where the energy is eventually dissipated as heat. The planetary boundary layer within which this frictional loss occurs may be considered to consist of two parts: a surface layer about 2 m thick just below the ice, and, below that, an Ekman layer about 25 m thick. Observations are concentrated in the Ekman layer although not restricted to it. The planetary boundary layer in the Arctic Ocean is much more accessible than the atmospheric boundary layer which has a height of several hundred meters extending well above the reach of meteorological towers on the ice. However in the ocean it is relatively easy to deploy instruments through the relatively thin oceanic boundary layer to measure the momentum change in a fairly complete manner. Advantage is taken of this fact in the AIDJEX field studies. Stress is calculated with a momentum integral technique (Hunkins, 1975a). When conditions are relatively steady there will be a balance between five different horizontal forces acting on the pack ice. The driving force is exerted on the upper ice surface by the wind. On the lower ice surface there is drag force exerted by the water. In addition there are body forces acting on the ice. The Coriolis force acts at right angles to the ice motion due to the earth's rotation. There is a pressure-gradient force caused by the minute tilt of the sea surface. Finally since conditions vary from place to place on the ice pack there is an internal ice force. An example of the balance of forces on pack ice is shown in Figure 3 for the mean conditions over a 60-hour interval. The water stress was calculated by the momentum integral method and the air stress is based on wind observations. Coriolis force was calculated from the known ice velocity and unit mass. The pressure-gradient force was obtained from oceanographic observations. The internal ice force cannot be determined directly and is the equilibrating residual in this diagram. One of the objectives of the AIDJEX program is to provide better measures of the internal ice force.

Offsetting the observational advantage of shallow depth in the oceanic boundary layer is the fact that the keels of pressure ridges may on occasion extend through an appreciable fraction of the planetary boundary layer. This presents a sampling problem since there are not enough instrument arrays to sample statistically in space. Representative instrument sites were selected, and the keel drag will be assessed separately and coupled with ridge frequency statistics. It will be necessary to

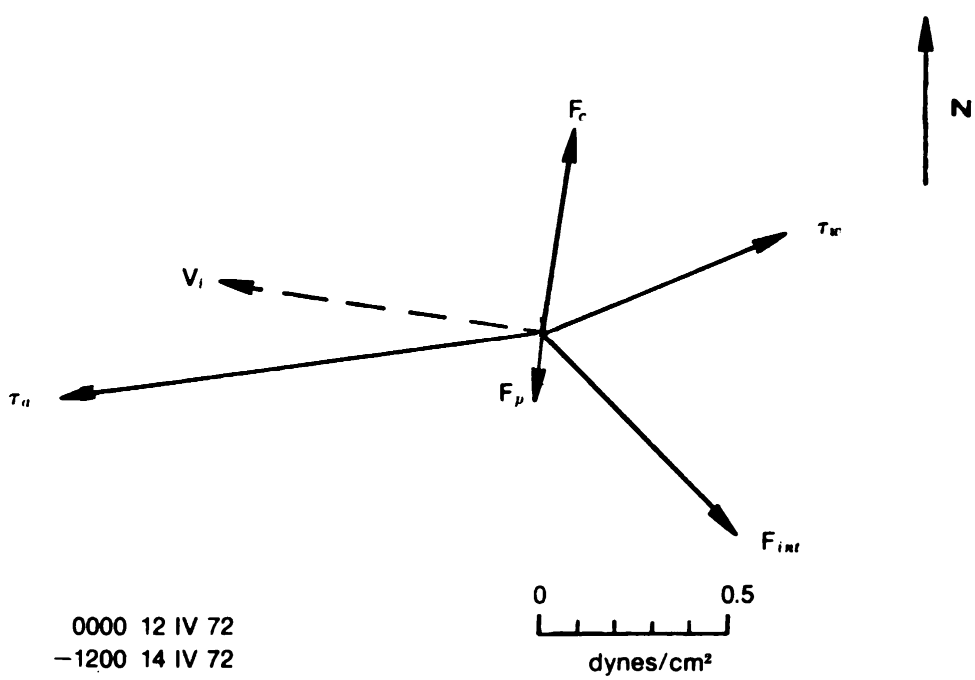

Figure 3 — Mean balance of forces on the pack ice at the main camp of the AIDJEX pilot program for April 12-14, 1972.

provide average drag coefficients for the underside of the ice for use in the computer models and progress is being made in this direction (Hunkins, 1975b.)

The ice provides a stable platform for instruments and permits the study of some fundamental oceanographic phenomena in a way not possible in the open ocean. Fundamental oceanographic discoveries have been made in the Arctic Ocean and we can hopefully assume that more will be made in the future. It was in the Arctic Ocean that Nansen, in his expedition on the *Fram*, (1893-96) first observed that ice drifts to the right of the wind direction. These observations stimulated Ekman's theory of boundary layers in which both friction and the earth's rotation are important. The theory is still one of the cornerstones of oceanography. Internal waves were also first observed by Nansen on the same expedition.

The main AIDJEX experiment will sample many phenomena of basic oceanographic importance. Observations from the manned stations will provide a one-year set of data over a 100 km array. Systematic data on currents, temperature, and salinity from arrays of any scale are rare in the oceans. There is no world network of continuous observational stations for the oceans such as the meteorologists have for the atmosphere. It has become increasingly evident that time-dependent motions are important to ocean circulation and mixing. The AIDJEX array provides a unique opportunity to study motions with horizontal scales of 100 km, vertical scales of 1000 m or less, and time scales of less than one year.

Some of the phenomena investigated, such as mixed layer dynamics, relate directly to the stress problem. The mixed layer is well developed in winter and spring by brine convection induced by the freezing ice sheet. Conditions change in the summer as meltwater empties into leads and holes through the ice to produce a statically stable water column. Summer conditions are little known and the effect of stable conditions on water stress is still undetermined. In addition to the flux of momentum, the fluxes of mass, heat, and salt in the mixed layer will be determined. The horizontal mass flux in the mixed layer may be measured directly over the array and checked against indirect mass divergence calculations based on the stress observations. If the observations of stress differences over the array are sufficiently accurate it will be possible to measure stress vorticity which should balance mass divergence in the Ekman layer. Mass divergence found independently from mixed layer thickness can thus provide a check on the direct stress observations.

It is to be expected that in a large and carefully planned experiment such as AIDJEX, interesting and unusual phenomena will occur from time to time which had not been fully anticipated by the planners.

Such were the transient undercurrents, attaining speeds of 40 centimeters per second at a depth of 150 meters, which were noted on certain occasions. Although similar motions apparently have been observed a few times before in the Arctic Ocean, they were not observed in either the 1970 or the 1971 pilot programs.

Baroclinic eddies in the Arctic Ocean were first clearly documented during the 1972 AIDJEX pilot study (Hunkins, 1974; Newton et al., 1974). The eddies have diameters of 10-20 km with current speeds reaching 45 cm/sec. They are restricted to a limited depth range between 50 and 300 m. The Arctic eddies contrast with those in other oceans which generally have a larger diameter and a surface, rather than subsurface, maximum of horizontal velocity. An example of a vertical current profile through an arctic mesoscale eddy is shown in Figure 4. Note the maximum current of about 40 cm/sec at a depth of 150 m. The measured currents are based on both direct current meter observations and indirect geostrophic calculations. These eddies are observed to be roughly circular in plan and both clockwise and counterclockwise circulation has been noted. During periods of rapid drift during storms, the ice moves much faster than the eddy and observations can give a section through an eddy. An example is shown on Figure 5 where the current vectors at a depth of 100 m are plotted as the ice drifted across an eddy with a diameter of 10 km.

The differing properties of the Arctic eddies may be associated with the ice cover and with the steeper density gradient there. If so, the Arctic Ocean provides an opportunity on a geophysical scale to study eddies under altered conditions. The origin of these eddies and their part in the exchange of momentum, heat, and salt are not known with certainty. It is believed that they originate in the baroclinic instability associated with the mean shear between the Pacific and Atlantic Water Masses which intrude into the Arctic Ocean from opposite sides. If this theory proves correct, the Arctic Ocean eddies will be analogous to the weather systems of the atmosphere which are formed as a result of the instability of the mean wind shear generated by global temperature differences.

Before the role of eddies in large-scale mixing of heat, salt, and momentum can be understood, more statistics are needed on size and numbers. The AIDJEX results will help provide them. It may be possible to track one or more of these eddies across the array long enough to measure its decay rate. The array spacing was specifically designed to sample the synoptic meteorological scale since this is the scale of wind-driven ice drift. The eddy problem requires an array with a finer mesh, say, 5-10 km. Plans are being developed to deploy such an array in early 1976.

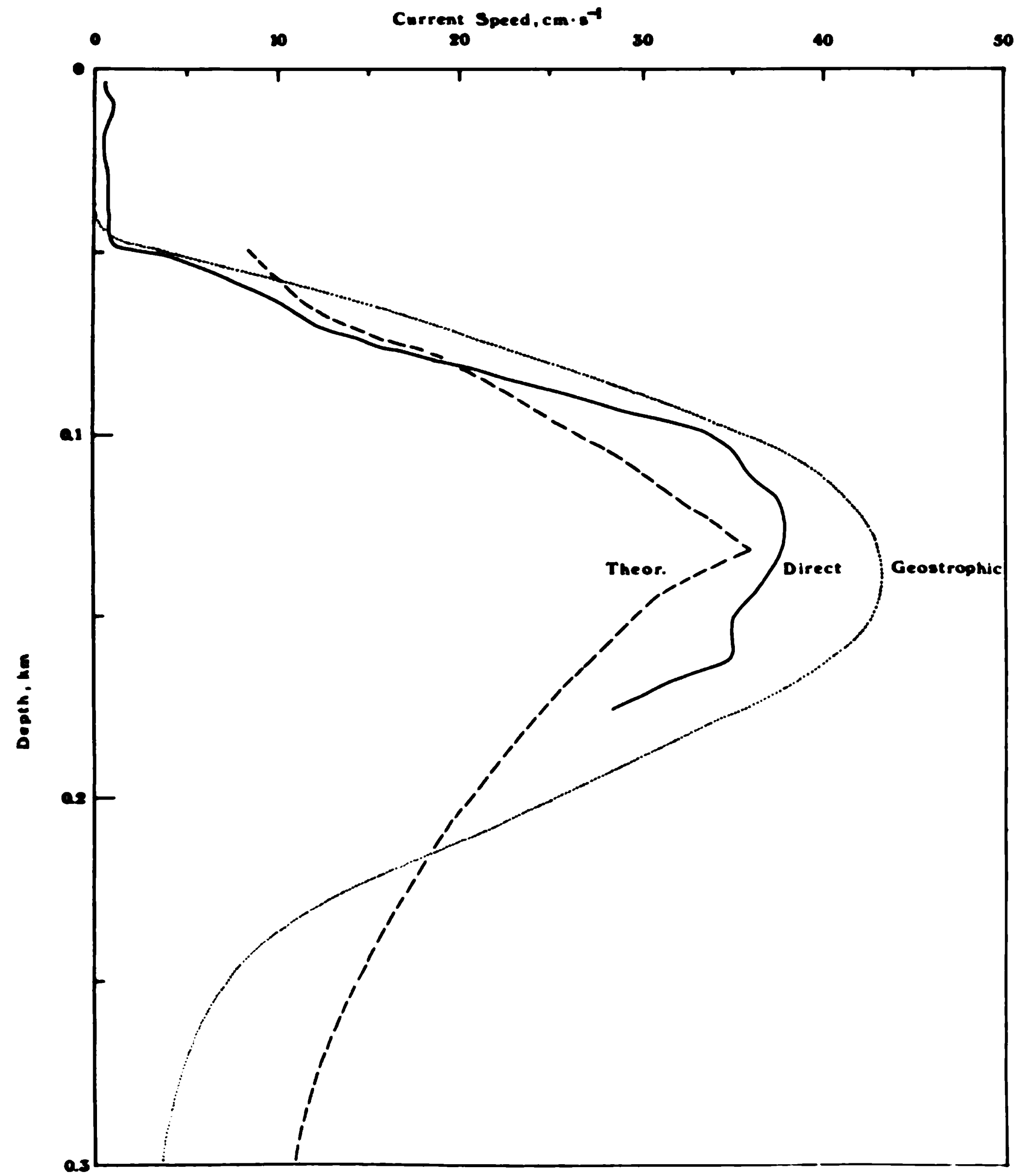

Figure 4 – Current profiles through an arctic mesoscale eddy. The solid line represents direct current meter observations, the dotted line represents calculated geostrophic velocities between closely-spaced salinity and temperature profiles, and the dashed line is based on a theoretical baroclinic instability model.

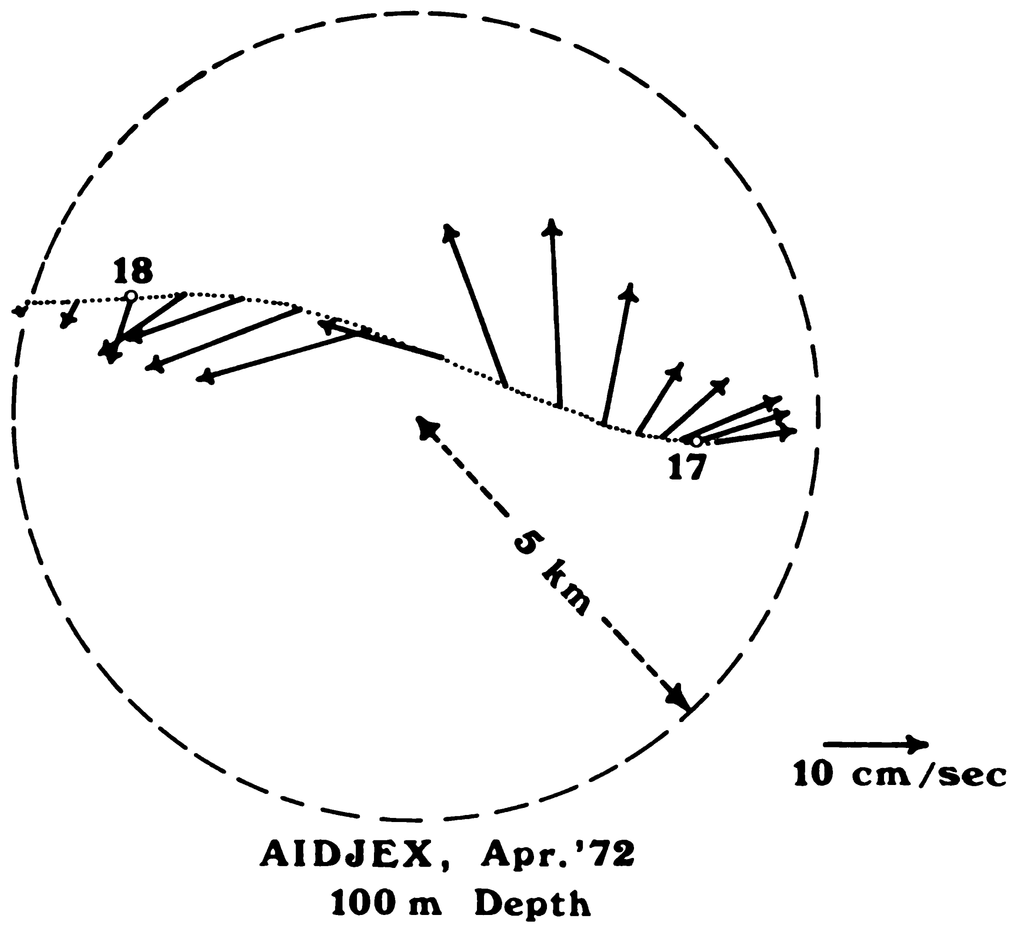

Figure 5 — Current vectors at 100 m depth across an arctic mesoscale eddy observed during rapid ice drift in April, 1972.

References

K. Hunkins, 1974a. "The Oceanic Boundary Layer and Ice-Water Stress During AIDJEX 1972." *AIDJEX Bulletin No. 26*, p. 109-127.

K. Hunkins, 1974b. "Subsurface Eddies in the Arctic Ocean." *Deep-Sea Research*, **21**, 1017-1033.

K Hunkins, 1975. The Oceanographic Program for the AIDJEX Main Experiment." *AIDJEX Bulletin No. 28*, p. 48-60.

K. Hunkins, 1975. Geostrophic Drag Coefficients for Resistance Between Pack Ice and Ocean." *AIDJEX Bulletin No. 28*, p. 61-68.

G. A. Maykut, A. S. Thorndike and N. Untersteiner. 1974. "Arctic Ice Dynamics Joint Experiment Scientific Plan." *AIDJEX Bulletin No. 15*, 67 pp.

J. S. NEwton, K. Aagaard and L. K. Coachman, 1974. Baroclinic Eddies in the Arctic Ocean." *Deep-Sea Research, 21*, p. 707-720.

W. Ruddiman and A. McIntyre, 1973. Time-Transgressive Deglacial Retreat of Polar Waters from the North Atlantic." *Quaternary Research, 3*, p. 117-130.

U. S. GOVERNMENT PRINTING OFFICE : 1976 O - 203-429

ATS Communication on Oceanographic Vessels—A Low-Cost Alternative to Shipboard Computers

Teletype, facsimile, and voice communication via satellite have proven valuable in several oceanographic experiments. A current effort to implement reliable data and command exchange between shipboard stations and land-based computer facilities promises to extend enormously the information processing capability available to oceanographic investigators at sea. At the Rosenstiel School of Marine and Atmospheric Science (RSMAS), University of Miami, Drs. Otis Brown and Robert Evans, with Mr. Paul Eden, Design engineer, are currently field testing a wideband, noise-insensitive duplex data transmission system using the ATS III satellite. Based on a PCM (pulse code modulated) encoding system which has been proven in several remote environmental data systems by the Divisions of Atmospheric Science and Physical Oceanography at RSMAS, their prototype station is currently installed on the R/V COLUMBUS ISELIN. Its first test in a real project situation during a profiler test cruise in the eastern Gulf of Mexico was successful. Data from several profiling and fixed-level sensors, recorded initially onboard ship, will be transmitted to the computer facility at RSMAS, processed, and returned to the shipboard investigators in facsimile graphic format, providing the experimenter with the basis for near-real time feedback in project execution.

Compared to the expense of maintaining shipboard computer systems, including seagoing support personnel, this approach is economically very attractive. At a cost per shipboard installation of approximately $30,000, access can be provided to considerably more complex and powerful computer equipment than one could reasonably carry at sea; and a single shore-based facility can service a substantial number of vessels or fixed field stations on islands or buoys. Incidentally, the system also provides superior general purpose ship-to-shore communication, including teletype, facsimile, and voice transmission, as well as ship-to-ship communication possibilities for the purpose of coordinating multi-ship operations.

NAVAL RESEARCH REVIEWS publishes highlights of research conducted by Navy laboratories and contractors and describes important naval experimental facilities. Manuscripts submitted for publication, correspondence concerning prospective articles, and changes of address, should be directed to Code 730, Office of Naval Research, Arlington, Va. 22217. Requests for subscriptions should be directed to the Superintendent of Documents, U.S. Government Printing Office, Washington, D.C., 20402. Subscription price: $6.50 per year in the U.S. and Canada; $8.15 per year, foreign; $0.55 per individual copy. The issuance of this periodical approved in accordance with Dept. of the Navy publications and printing regulations.

Editor: WILLIAM J. LESCURE

NAVSO P-510

Associate Editors:

A. R. LAUFER, ONR PASADENA

A. R. DAWE, ONR CHICAGO

A. L. POWELL, ONR BOSTON

D. A. PATTERSON, NAVAL RESEARCH LABORATORY

IN THIS ISSUE

VOL. XXIX, NO. 3

Cover Caption

Methods used to evaluate temperature anomaly patterns in the ocean. The P-3 aircraft is shown dropping AXBT's (airborne expendable bathythermographs) along one of the flight paths between Hawaii and Alaska. Also indicated are the drifters; these buoys record temperature data which is then transmitted via satellite to various shore facilities for analysis. The lines in the ocean's cross section indicate the temperature patterns. *See page 36.*

DEPARTMENT OF THE NAVY
OFFICE OF NAVAL RESEARCH
ARLINGTON, VA. 22217

OFFICIAL BUSINESS

PENALTY FOR PRIVATE USE, $300.

POSTAGE AND FEES PAID
DEPARTMENT OF THE NAVY
DoD-316

U.S.MAIL